Wind Optimization of Flight Profiles through the Reykjavik Control Area

Ninna Björg Ólafsdóttir

Thesis of 30 ETCS credits
Master of Science in Engineering Management

June 2014

Wind Optimization of Flight Profiles through the Reykjavik Control Area

Ninna Björg Ólafsdóttir

Thesis of 30 ECTS credits submitted to the School of Science and Engineering
at Reykjavík University in partial fulfillment of
the requirements for the degree of
Master of Science in **Engineering Management**

June 2014

Supervisors:

Þorgeir Pálsson, Sc.D., Supervisor
Professor, School of Science and Engineering at Reykjavík University

Eyjólfur Ingi Ásgeirsson, Ph.D., Co-Supervisor
Assistant Professor, School of Science and Engineering at Reykjavík University

Hjalti Pálsson, M.Sc., Co-Supervisor
Manager of R&D ANS Division, Isavia

Examiner:

Jón Ágúst Þorsteinsson, Ph.D., Examiner
Chairman of the board, Marorka ehf.

Wind Optimization of Flight Profiles through the Reykjavik Control Area

Ninna Björg Ólafsdóttir

30 ECTS thesis submitted to the School of Science and Engineering
at Reykjavík University in partial fulfillment
of the requirements for the degree of
Master of Science in Engineering Management.

June 2014

Student:

Ninna Björg Ólafsdóttir

Supervisors:

Þorgeir Pálsson, Sc.D.

Eyjólfur Ingi Ásgeirsson, Ph.D.

Hjalti Pálsson, M.Sc.

Examiner:

Jón Ágúst Þorsteinsson, Ph.D.

The undersigned hereby grants permission to the Reykjavík University Library to reproduce single copies of this project report entitled **Wind Optimization of Flight Profiles through the Reykjavik Control Area** and to lend or sell such copies for private, scholarly or scientific research purposes only.

_____

Date

_____

Ninna Björg Ólafsdóttir
Master of Science

Wind Optimization of Flight Profiles through the Reykjavik Control Area

Ninna Björg Ólafsdóttir

June 2014

Abstract

Fuel efficiency has become an increasingly important factor in the aviation industry. The main reason is that fuel is the largest part of airlines operating expenses. Furthermore there has been increased awareness of the impact of man-made climate changes. The adoption of new aircraft fleets that are more fuel efficient can take decades. Operational improvements are however an effective way of improving fuel efficiency and environmental performance in the near term. Increasing fuel efficiency by optimizing aircraft tracks is an example of an operational improvement technique.

In this study an optimization algorithm that finds the shortest path in terms of time of flight for aircraft in the cruise phase was designed and implemented. The algorithm finds the most fuel efficient routes by taking advantage of accurate knowledge of wind direction and wind speed. The focus was on flights within the Reykjavik Air Traffic Control Area, where the effects of the North Atlantic jet stream were relatively strong. The results showed promising potential for improvements in lateral trajectory optimization where all the flights optimized showed some potential for fuel burn and thereby emissions to be reduced. Furthermore, the lateral trajectories were optimized 1,000 feet above and below the actual flight level. The results showed that there is a significant change in fuel consumption per minute between cruising altitudes, where the fuel consumption decreases with increased altitude. Therefore, although the highest cruising altitude resulted most often in the highest traveling time, the total fuel burn was always the lowest when the highest altitude was chosen. As the aviation industry is a large scale industry only a small rate of fuel burn reduction, like the one achieved in this study, can add up to substantial amount of fuel burn reduction and thereby CO_2 emission savings.

This research project was supported in part by a grant from Isavia.

Keywords: Fuel efficiency, Optimization, BIRD, Flight trajectories, Shortest path.

Bestun Flugferla með tilliti til Vinda í gegnum Flugstjórnarsvæði Íslands

Ninna Björg Ólafsdóttir

júní 2014

Ágrip

Nýting á eldsneyti er sífellt að öðlast meira vægi í flugiðnaðinum. Aðalástæðan er sú að eldsneyti skipar stærsta hluta rekstrarkostnaðar flugfélaga. Þar að auki hefur vitund um loftslagsbreytingar af mannavöldum aukist mjög seinustu ár. Þróun og innleiðing umhverfisvænni flugvélaflota, sem nýtir eldsneyti betur, getur tekið áratugi. Umbætur í rekstri, með bestun flugferla, er aftur á móti skilvirk leið til að bæta eldsneytisnýtingu og umhverfisáhrif í náinni framtíð.

Í þessari rannsókn var leitaralgrími þróað, sem finnur stystu flugleiðina með tilliti til tíma fyrir flugvélar í láréttu plani. Leitaralgrímið nýtir nákvæma þekkingu um vindátt og vindhraða til að finna flugferla sem lágmarka eldsneytiseyðslu og útblástur. Áhersla var lögð á að finna flug sem flugu í gegnum íslenska flugstjórnarsvæðið á dögum þar sem sterkir vindar blésu á Norður Atlantshafinu. Niðurstöðurnar sýndu að hægt er að bæta flugtíma með bestun flugferla í láréttu plani. Öll flugin skiluðu einhverri bætingu í flugtíma en bætingin var aftur á móti mjög misjöfn milli fluga. Bætingin í flugtíma var svo notuð til að finna það magn af eldsneyti og jafnframt það magn af CO_2 útblæstri sem sparast.

Flugferlar voru einnig bestaðir 1,000 fetum fyrir ofan og neðan raunverulega flughæð. Niðurstöðurnar sýndu að eldsneytiseyðslan lækkar með hækkandi flughæð. Þar af leiðandi, þó að hæsta flughæðin skilaði sér oftast í lengstum flugtíma þá var eldsneytiseyðlan alltaf lægst þegar hæðsta flughæðin var valin. Þar sem að flugiðnaðurinn er gríðarlega stór skilar aðeins smávægileg bæting í flugtíma, eins og sú sem náðist í þessari rannsókn, gríðarlegum heildar sparnaði í eldsneyti og þar með minnkun í CO_2 útblæstri.

Verkefnið var styrkt að hluta með sérstöku fjárframlagi frá Isavia.

Lykilorð: Eldsneytiseyðsla, Bestun, Flugferlar, Flugstjórnarsvæði, Leitaralgrími.

Acknowledgement

I would like to thank my supervisor Þorgeir Pálsson, for his guidance and support through the course of the thesis. I would also like to thank my Co-Supervisor, Eyjólfur Ingi Ásgeirsson, for his excellent guidance in the optimization part of the thesis.

I thank Isavia for supporting this project financially and for providing the flight data, along with the BADA fuel consumption model. Hjalti Pálsson, Head of Project Development Office at Isavia, my contact person at Isavia, receives special thanks for his input in the thesis and for his help in providing information related to the thesis.

Belgingur the Meteorological Research Institute and its owner and director Ólafur Rögnvaldsson I would like to thank for providing the weather data necessary to perform the study.

Table of Contents

List of Figures

List of Tables

Chapter 1

Introduction

Improving aircraft fuel efficiency has become an increasingly important factor in air transportation. The main reason is that fuel is the largest part of airlines' operating expenses, forecasted to be around $210 billion for the global airline industry in 2014, which equals 30 percent of the total operating expenses [1]. This is almost 5 times more than in 2003 when the fuel bill was around $44 billion for the global airline industry, which accounted for 14 percent of airlines' total operating expenses. Furthermore, fuel price has been rising in recent years and is expected to continue to rise in coming years [2]. The main reason is the growing demand for fossil fuels which has led to some concerns about the future of the world´s energy supply. This concern has driven up the cost of petroleum in a trend that is expected to continue.

Another reason for the emphasis on flight efficiency is increased awareness of the impact of man-made climate changes and the introduction of the European Union of carbon charges, which leads to an additional cost item for airlines, which is the emission of greenhouse gasses (GHG). Aviation accounts for around two percent of global man-made CO_2 emissions [3]. Moreover, emissions from air transport are growing faster than from any other mode of transportation as other modes are more easily adapted to environmentally sustainable practices and environmentally friendly techniques. Furthermore, air transportation is growing around five percent a year which emphasizes the importance of minimizing aircraft fuel [4].

As fuel price increases, aircraft operators must put more effort into finding margins for improvement in aircraft performance. Increased awareness of the impact of man-made climate changes has resulted in pressure from the government and international agencies to reduce fuel consumption, as they have set goals for future emission reduction. These factors have resulted in increased effort to improve aircraft fuel efficiency, however the effort needed to make more fuel efficient aircraft fleets is enormous as the process is extremely slow and expensive [5]. The adoption of new aircraft fleets that are more fuel efficient can take decades. Operational improvements are however an effective way of improving fuel

efficiency and environmental performance in the near term. Increasing fuel efficiency by optimizing aircraft tracks is an example of an operational improvement technique.

This study was carried out in collaboration with Isavia, the provider of airport and air navigation services in Iceland. Minimizing aircraft fuel and thereby emission is not only in the interest of airlines but also air navigation service providers, like Isavia. In recent years Isavia has been active in projects that emphasize the reduction of aircraft fuel burn and CO_2 emissions in the North Atlantic Region. The European Union charges air traffic for emission, so service providers are now being pressured to define routes that lessen fuel consumption within their area of responsibility. Air Traffic Control (ATC) Centers therefore try not to specify fixed routes that aircraft have to follow; rather they collaborate with the airlines to find the most efficient routes, that minimize fuel consumption and thereby CO_2 emission.

1.1 Research Goals

This research attempts to accomplish the following goals:

1. Design and implement an optimization algorithm that will find the shortest path in terms of time of flight for aircraft in the cruise phase.
2. Determine to what extent fuel burn of jet transport aircraft can be reduced by taking advantage of improved estimates of the wind conditions encountered at jet altitude flight levels.

The main benefit of this research will be the development of a wind optimization (WO) algorithm that will find the most fuel efficient routes by taking advantage of accurate knowledge of wind direction and wind speed. The emphasis will be on minimizing fuel consumption in the aircraft cruise phase, as this is by far the longest segment of flight in the North Atlantic Region and occurs between the climb and descent phases [6]. The oceanic part of the cruising phase usually consists of a constant airspeed and altitude; the only factor that changes is the heading of the aircraft, although there can be occasional changes in altitude.

The focus will be on flights within the Reykjavik Air Traffic Control Area (BIRD). Isavia will potentially be able to use this model to find the most fuel efficient routes for aircraft that fly within BIRD and use the WO model to demonstrate the efficiency of Air Traffic Management

(ATM) procedures by advising operators of potential improvements in flight planning. This approach can possibly lead to tactical improvements in air traffic control whereby lateral modifications of the track flown would be undertaken on the fly, i.e. by deviating from the planned track.

Based on previous research [7], it is assumed that 1-2% fuel burn reduction can be achieved by using wind optimal routes instead of routes that were established by the flight plan generated in the conventional way prior to departure. A 1% fuel burn reduction would result in significant economic benefits. Based on 2013 traffic figures, the number of flights that flew within BIRD in 2013 was 116,326 [8]. As the average time spent within BIRD is 100 minutes, the total time spent within the area was approximately 11,632,600 minutes in 2013. A 1% fuel burn reduction would result in approximately 1,940 fewer hours spent within BIRD. This would result in roughly 6,250 metric ton fuel savings annually, based on 2013 traffic figures. The price for a metric ton of jet fuel in May 2014 was around $963 [9]. Based on this price the economic saving would amount to approximately $6.02 million per year. Furthermore the air traffic within BIRD has been increasing on average of 4.15% annually for the last ten years [8] and the price of jet fuel has been rising in recent years and is expected to continue rising in coming years. These figures emphasize the importance of operational improvements and the substantial economic benefit they can lead to.

Emphasis was placed on finding flights where the effects of the North Atlantic jet stream are relatively strong. This was done in corporation with Isavia and the Institute for Meteorological Research (IMR). The North Atlantic jet stream are strong westerly winds that usually exceed 30 meters per second (m/s), although the wind speed can be as high as 107 m/s [10]. The North Atlantic jet stream generally moves from west to east, although its path typically has a meandering shape where the jet stream curves north and south [11]. Figure 1.1 shows the mean jet stream effect at 34,000 feet on 9th of October 2013. The jet stream meandering shape can be seen clearly in the figure. The wind speed is in meters per second and as can be seen ranges from under 10 m/s up to over 60 m/s. Aircraft flying from North America to Europe tend to exploit the strong tail wind created by the jet stream while aircraft flying from Europe to North America try to minimize the impact of the headwind by adjusting the flight profile.

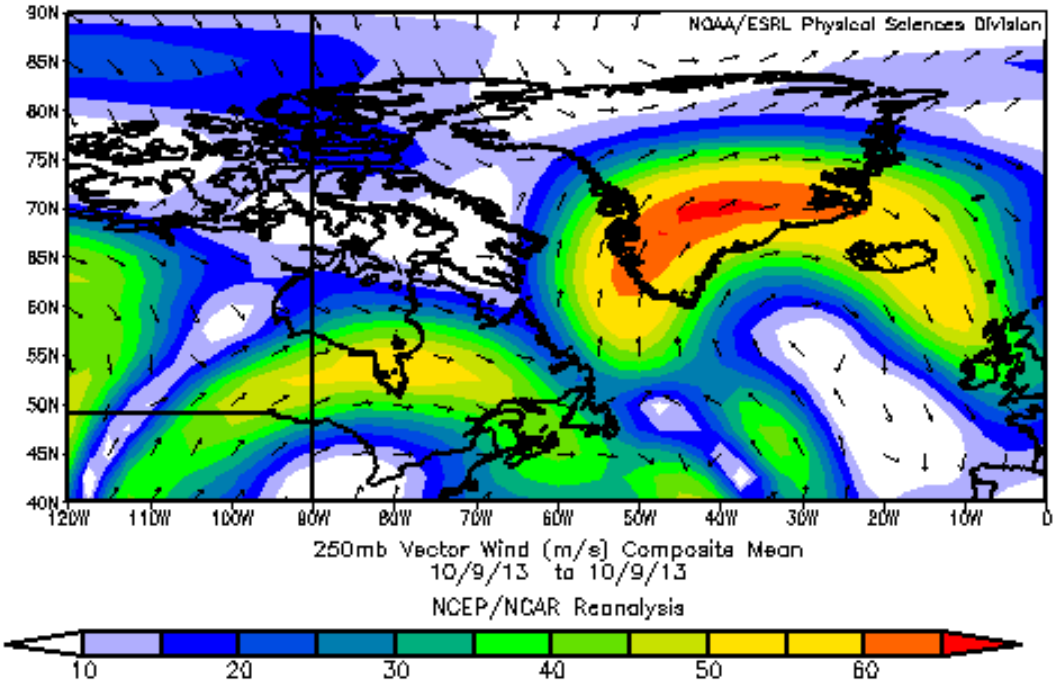

Figure 1.1: The mean vector wind in meters per second at 34,000 feet on 9th of October 2013 [12] .

Literature review revealed that extensive research has been done in the field of aircraft track optimization [13, 14, 15]. Numerous optimization algorithm models have been developed that find the most fuel efficient routes. However the aviation industry is a very commercially competitive industry. Therefore it is hard to obtain all the data needed to perform such a study as both reliable flight data and accurate weather data are needed. This research was done in collaboration with Isavia, which provided all the flight data needed, and also the Institute for Meteorological Research (IMR) that provided all the weather data needed to perform the study.

1.2 Research Overview

In this research fuel efficiency will be attained by considering lateral optimization of the flight profile whereby the most efficient flight trajectories will be determined with respect to up-to-date information on winds aloft. In Chapter 2 the Reykjavik Control Area will be introduced. Technological developments in this field will be discussed along with other research that has been undertaken on this subject. The algorithm used in this study will be introduced and the

great circle distance will be explained. Finally, the concepts of airspeed and ground speed will be explained. In Chapter 3 both the flight data obtained from Isavia and the weather data obtained from IMR is presented along with the flights chosen for the optimization. In Chapter 4 the WO model is established and explained along with the computations used. Moreover the BADA model will be introduced. In Chapter 5 the accuracy of the WO model and the BADA model will be discussed and furthermore the quality of the weather data is addressed. Chapter 6 will present the wind optimization results. Finally, the conclusions are presented in Chapter 7 along with recommendations for future research.

Chapter 2

Background

The air transportation industry is a very commercially competitive industry, which also makes it a low margin industry. Operating improvement techniques which lower the operating cost are therefore especially important for the aviation industry. Operational strategies like altering the flight profile are an effective way of improving fuel efficiency in the near term. However, flying the most efficient flight profiles often leads to reduced aircraft separation, which makes surveillance of the air traffic more complicated. The international airspace is governed by International Civil Aviation Organization (ICAO) [16]. The ICAO delegates the responsibility for air traffic control and other air navigation services within the North Atlantic airspace to seven states: The United Kingdom, Canada, Norway, USA, Denmark, Portugal and Iceland.

2.1 Reykjavik Control Area

Isavia has responsibility for Air Traffic Management Services in the Reykjavik Flight Information Region (FIR) and the Sondrestrom Flight Information Region [16]. These areas can be seen in Figure 2.1. The Reykjavik FIR and the Sondrestrom Flight Information Region are known as the Reykjavik Control Area (CTA) or, by the ICAO identifiers as BIRD CTA, often referred to as BIRD. The area is about 5.4 million square kilometers and covers territory from the boundaries of Russian, Norwegian, British/Irish, Shanwick and Canadian airspace. The Reykjavik CTA is divided into smaller geographical areas, referred to as sectors, in order to facilitate the control of the air traffic. Four sectors have been defined in the Reykjavik CTA; these are the North, West, South and East sector as shown in Figure 2.2.

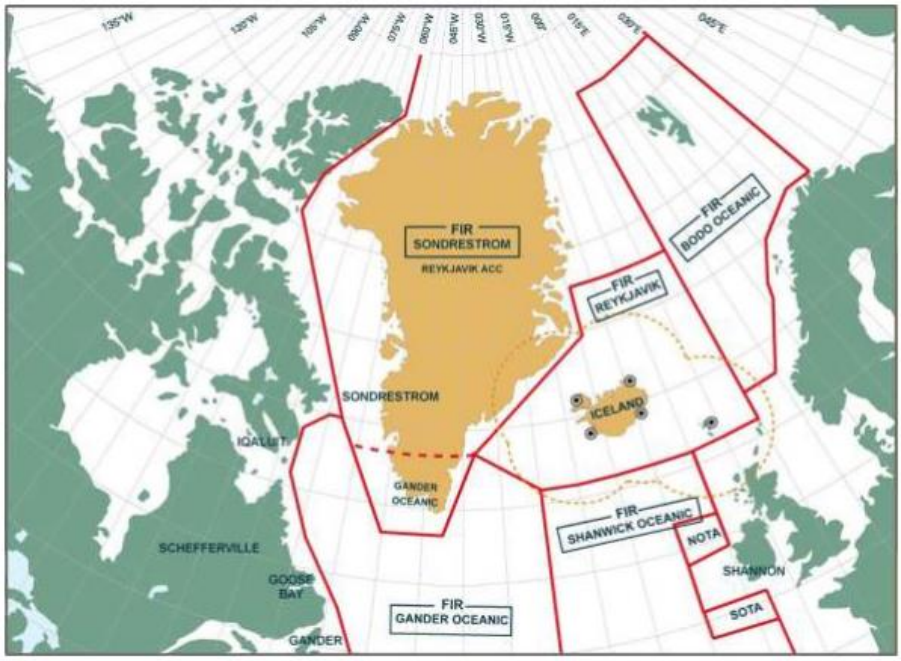

Figure 2.1: The Reykjavik FIR and the Sondrestrom FIR [17] .

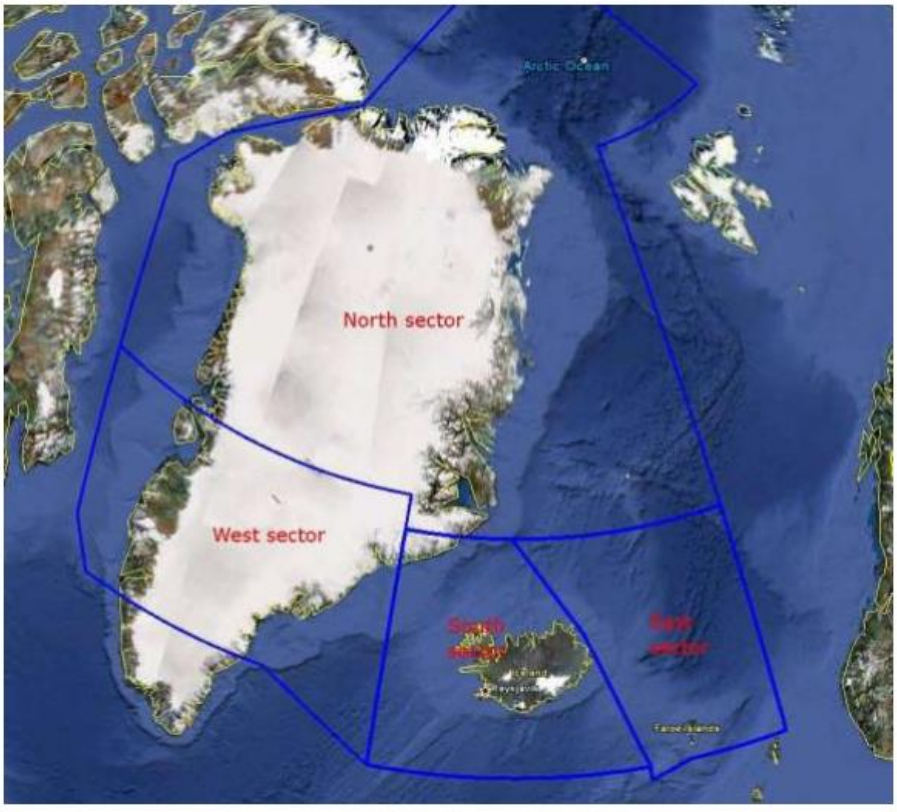

Figure 2.2: The North, West, South and East sector of the the Reykjavik CTA [16].

2.2 Technological Developments

In recent years new systems have been developed that make surveillance and communications easier than in the past. Also information networks have been established, enabling the sharing of critical operational data between aircraft and ground stations. These technological developments have improved both the efficiency and safety of flight. An example of these new systems is found in the implementation of Automatic Dependent Surveillance-Broadcast (ADS-B), which is a new technology used for surveillance of air traffic, in some instances replacing traditional radar surveillance [18]. ADS-B equipped aircraft transmit their position at short intervals on the radio frequency of 1090 MHz used by Secondary Surveillance Radars (SSR). The signal can be received by other aircraft, Air Navigation Service Providers (ANSP) or anyone that owns an ADS-B receiver. ADS-B therefore increases safety by making aircraft visible to other ADS-B equipped aircraft and to ANSP with position data transmitted typically once every second. ADS-B will be replacing radar as a surveillance method as it gives much more frequent and accurate update of the aircraft´s position. Isavia is now in the process of installing and putting into operation eight ADS-B receiver stations in Iceland, four in Faroe Islands and ten in Greenland. This process should be finished by the end of 2014. The ADS-B receiver stations in Greenland will for the first time introduce surveillance service in Reykjavik CTA West sector. The area within the solid blue line in Figure 2.3 represents the area of Isavia´s surveillance service when the new ADS-B receiver stations have been put into operation. This new surveillance service leads to a new era in air traffic control as aircraft will be able to cross the Atlantic Ocean within contiguous surveillance coverage. This system will allow for reduction of aircraft separation and therefore reduce the constraints that have the effect of reducing aircraft fuel efficiency. This will lead to increased fuel efficiency and reduction of CO_2 emission. The percentage of aircraft that are ADS-B equipped has increased steadily in recent years. Thus 70% of all aircraft transiting through the Reykjavik CTA in October of 2011 were transmitting valid ADS-B signals for use by ATC.

Data links between aircraft and ATC centers is another example of a technological development that has improved flight safety [19]. Data links carry flight information and instructions sent between aircraft and ground stations in the form of data rather than voice communication messages. The main advantage is improved safety as the chance of misunderstanding is lessened while at the same time the pilot and controller have time for other tasks. Around 50-60% of transatlantic flight traffic is now data link enabled [20]. It is

very important that the major part of the transatlantic flight traffic is data link enabled as over the North Atlantic there is little or no radar coverage and VHF radio contact is possible only over or near land masses, i.e. Iceland , Greenland and the Faroe Islands [19].

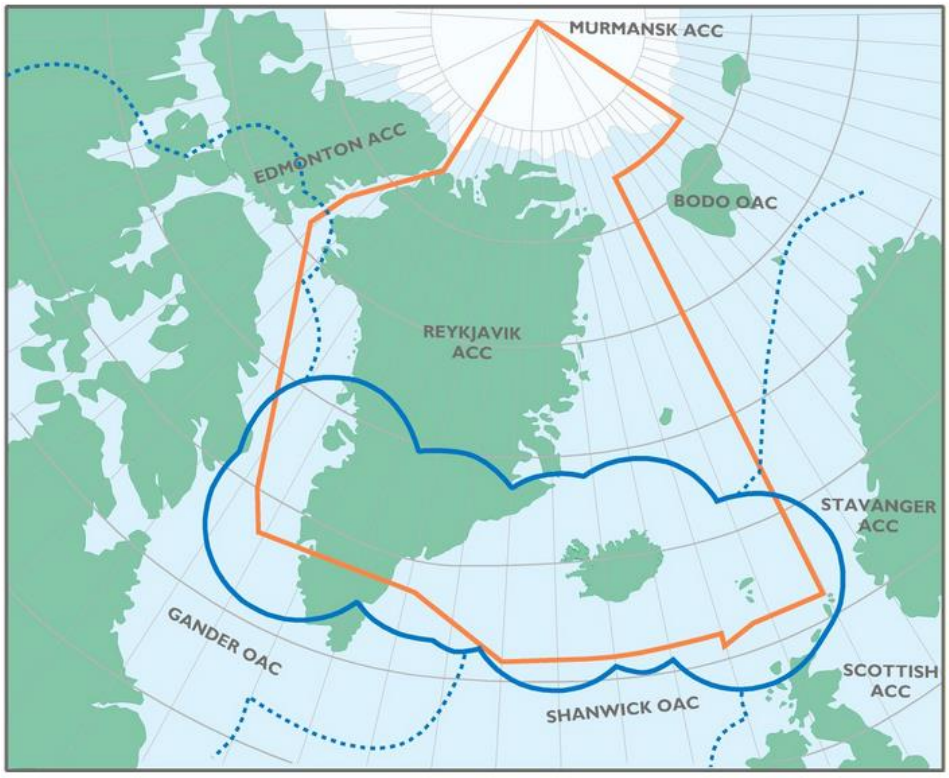

Figure 2.3: Isavia´s new surveillance corridor [18].

Automatic Dependence Surveillance Contract (ADS-C) [21] is a surveillance technique in which aircrafts automatically provide data derived from on-board navigation and position-fixing systems, including aircraft identification, four-dimensional position and additional data as appropriate. The data is however only provided on request where a data link is used. One of the difference between ADS-B and ADS-C is that ADS-C can only be initiated by registered users. Specific ADS-C messages may contain meteorological information obtained from the Flight Management System (FMS). However the ADS-C messages only contain meteorological information when asked for. Both temperature and wind observations are based on direct read outs from the FMS.

Recently ANSP have started to focus on finding the most efficient trajectories for the airlines. The UK service provider, NATS, is a leading player in this area [22]. NATS has established a special efficiency score, referred to as the 3Di score, that is used to assess the flight efficiency

and at the same time maintaining a high level of safety. ATC in this instance does not specify fixed routes that aircraft have to follow; rather they collaborate with the airlines and try to find the most efficient routes, e.g. direct great circle routes to minimize fuel cost and thereby CO_2 emission.

2.3 Previous Work

Various projects have been carried out with the goal of maximizing fuel efficiency and minimizing CO_2 emissions through optimized flight profiles. Reduction of Emissions on the North Atlantic by the Implementation of ADS-B is a project that was carried out by Isavia in 2009-2010 [13]. This project was supported by the SESAR Joint Undertaking under the so called AIRE (Atlantic Initiative for the Reduction of Emissions) program. Icelandair, in cooperation with Isavia, conducted flight trials to test the feasibility of improving fuel efficiency in the Reykjavik CTA. This was carried out by pursuing more optimal flight profiles using direct routing, cruise-climb and variable speed within the future ADS-B North-Atlantic Surveillance Corridor in the Reykjavik CTA. Estimated benefits from these procedures were most significant for direct routing, i.e. around 0.2%-0.7% of the total fuel burn. The results showed also that the trial installation of ADS-B receiver stations in Greenland would increase the surveillance duration of the aircraft track from 55% to 85% of the total distance along this route. The fuel burn estimates were obtained using the BADA (Base of Aircraft Data) model that has been developed and maintained by Eurocontrol through collaboration with operating airlines and aircraft manufactures [23]. The data and information contained in BADA is designed for use in aircraft track predictions and simulations. This Aircraft Performance Model (APM) has been implemented in Matlab for simulation usage by Isavia and Tern Systems as described further in Chapter 4.5.

Dynamic Optimization of the Route In flight at Santa maria (DORIS) is a dynamic optimization project that was performed during the year 2011 [14]. DORIS was a collaboration project between the partners Iberia, Air Europa, Air Portugal and INECO and the subcontractors AESA and SENASA. The flights transiting through Santa Maria FIR and New York Oceanic FIR were used. The Iberia and Air Europa airlines operate several long haul flights that cross the Santa Maria and New York Oceanic FIRs, these flights were used in the DORIS project. Iberia´s flights were optimized with respect to fuel and time savings while

Air Europa´s flights were only optimized with respect to fuel savings. The main goal of the DORIS project was to reduce fuel consumption and environmental impact. This was carried out by tested and validated techniques for the efficiency improvement in oceanic airspace flight trajectories. The main thrust of the DORIS project was finding optimized routes using updated weather forecasts instead of planning the flight routes several hours ahead of flight departure, like airlines usually do. A dynamic optimization was therefore used as new flight plans were calculated in-flight using the most up-to-date meteorological information. These procedures resulted in average savings of 2.5% of the total fuel consumption and CO_2 emissions per flight, compared to the estimated fuel burn of the flight track originally planned.

Cross-Polar Aircraft Trajectory Optimization and the Potential Climate Impact is a research study that was undertaken by NASA Ames Research Center in 2011 [15]. In this study an optimization algorithm is generated that finds wind optimal aircraft tracks for cross-polar flights, that minimize the impact of climate changes, in terms of global warming potential (GWP). This study only considers the GWP for CO_2, NO*x* and H_2O emissions but these emissions are converted into GWP figures using specific conversion factors. The aircraft deviate from fixed routes with the aim of reducing environmental emissions by minimizing fuel burn. The great circle and wind optimal trajectories for cross-polar flights between three origin-destination city pairs were analyzed. Results showed that wind optimal routes have about 0.3% to 2% fuel saving when compared to the great circle routes. When trajectories between Chicago and Hong Kong were analyzed, results showed that the wind optimal routes have the highest global warming potential savings at all flight levels when compared to the flight plan trajectories and that aircraft flying at higher altitudes produce smaller global warming potential. Finally, two days were analyzed for cross-polar flights between 15 origin-destinations city pairs. Using the wind optimal routes reduced average fuel burn and GWP by 8.0% on August 7, 2010 and 4.4% on December 4, 2010, compared to that of flight plan routes.

This research is a follow up of an MS project that was carried out by Einar Ingvi Andrésson in 2012 titled Lateral Optimization of Aircraft Tracks in Reykjavik Air Traffic Control Area [7]. In this project fuel burn and emissions were minimized by optimizing flight trajectories with respect to “actual” or “true” wind. The optimization algorithm used was a Dijkstra search algorithm which calculates the shortest path in terms of time of flight for aircraft in the cruise phase. Only two flights were examined in this study, both of which were flown during the

summer. The first flight was from Keflavik to New York and the second flight was from Keflavik to Copenhagen. Both of these flights resulted in close to 1% fuel burn reduction when compared to the fuel consumption estimated for the cruise phase by the flight plan.

The former study only considered two flights, which both where flown during the summer, however in this current study more flights are considered and emphasis is placed on finding flights where the effects of the North Atlantic jet stream effect are relatively strong. Furthermore the two flights examined only flew in part of the BIRD whereas in this study all the flights examined fly all the way through the area. The former study used a rather simple grid, used to deviate from the planned flight track, as in this current study a more practical grid will be constructed, which is easy to change and adapt in order to achieve maximum improvement. Furthermore, validation of the accuracy of the estimated actual wind conditions is emphasized in this current study.

2.4 The Algorithms considered for the Optimization

Optimization problems can have many possible solutions [24]. Each solution has a value and the goal is to find the optimal value. The optimal value is either the minimum or the maximum value and is called an optimal solution. In this study an optimization algorithm is generated that finds the shortest path in terms of time for aircraft in the cruise phase. Therefore the goal is to find the minimum traveling time. An algorithm is any computational procedure that takes some value, or often a set of values, as input and transforms the input into some value, or set of values, as output. The WO problem takes data from various sources as an input and produces the output, which is the minimum traveling time.

Several algorithms have been developed to solve optimization problems, for example dynamic programming, genetic algorithm and depth-first search [24]. There are number of algorithms that are applicable to solve the shortest path problem. Several of these algorithms were considered when constructing the optimization model. The first algorithm considered was Dijkstra´s algorithm, which is one of the most common algorithms used for solving the shortest path problem. Dijkstra´s algorithm solves the single-source shortest-paths problem on a weighted directed graph and is only capable of handling graphs which all edge weights are nonnegative. In this optimization problem the edge weights can never be negative numbers as the heading of the aircraft is directed. The lack of feature of being capable of handling graphs

in which some of the edge weights are negative numbers is therefore not a problem in this optimization problem. Other algorithms for the shortest path problem include the Bellman-Ford algorithm. The Bellman-Ford algorithm solves the single-source shortest paths problem in the general case, it is capable of handling graphs where some of the edge weights are negative numbers. However, as mentioned above in this optimization problem the edge weights can never be negative numbers as the heading of the aircraft is directed. Furthermore, Dijkstra´s algorithm has shorter running time then Bellman-Ford algorithm when used to solve the same problem. Dijkstra´s algorithm has typically a running time of $O(|E| + |V|\log|V|)$ while the Bellman-Ford algorithm has a running time of $O(|V||E|)$, where $|E|$ is number of edges and $|V|$ is number of vertices. The Floyd-Warshall algorithm was also considered, this algorithm is also capable of handling graphs in which some of the edge weights are negative numbers, as Bellman-Ford algorithm. Moreover, Floyd-Warshall algorithm does not only compute the shortest path but rather it computes all possible paths. However as not every possible path is needed for this optimization problem, Floyd-Warshall algorithm may be a waste of time because too many unwanted shortest paths will be calculated. Calculating every possible path consequently results in a long running time. The running time of Floyd-Warshall algorithm is $O(|V|^3)$, which is obviously longer than the running time of Dijkstra´s algorithm. After considering these three algorithms it was concluded that Dijkstra´s algorithm is best suited for this optimization problem as the heading is directed and it results in the shortest running time.

2.2.1 Dijkstra´s Algorithm

An algorithm is a procedure that must solve a general, well-defined problem. Dijkstra´s algorithm is the primary algorithm to solve the shortest path problem, it is used to find the shortest path on a weighted, directed graph with n vertices from a given starting vertex to all $n - 1$ other vertices [25]. However Dijkstra´s algorithm only works for cases where the graph has no negative cost weights, which is not a problem in this optimization problem as the edge weights can never be negative numbers. A graph can be represented by using an adjacency matrix. An adjacency matrix has an equal number of rows and columns labeled by graph vertices with 1 in position (v_i, v_j) where vertices v_i and v_j are adjacent but 0 otherwise [26]. Given a graph G, and starting node s, Dijkstra´s algorithm finds the optimal path from the starting node s to all other nodes.

Following is the implementation of Dijkstra´s algorithm [24]:

DIJKSTRA (*G*, *w*, *s*)

```
1  Initalize single source (G, s)
2  Set S = ∅
3  Set Q = V[G]
4  While Q is not empty do
5        Set  u = EXTRACT-MIN(Q)
6        Set S = S ∪ {u}
7        for each vertex v ∈ G.Adj[u]
8            Relax(u, v, w)
```

Given an initial graph G, all nodes have infinite distance (cost) except the starting node, *s*, which has a distance of 0. S, which is the set of visited vertices, is initially empty while Q, the queue, contains all vertices. While Q is not empty a node from Q, which has the lowest distance from the starting node *s*, is selected and processed. Distances of all unprocessed descendants of the selected node are reevaluated. If the distance of the node which is being processed plus the edge weight from the node which is being processed to the descendant node is less than the current distance of the descendant, the distance of the descendant is updated and the processed node is set as his ancestor. *u* is then added to the list of visited vertices. If a new shortest path is found, the array of best estimates of the shortest path is updated, along with the array of predecessor.

Because Dijkstra´s algorithm always chooses the "closest" vertex in Q = $V - S$ to add to set *S*, it can be said that Dijkstra´s uses a greedy strategy [24]. In general, greedy strategies do not yield optimal results all the time; however it has been proved that Dijkstra´s algorithm does indeed always find the shortest path.

2.5 Great Circle Distance

The Great Circle Distance (GCD) is the shortest distance between any two points on a surface of a sphere [27]. The great circle distance can be computed from the latitudes, which are represented by δ, and longitudes, which are represented by λ, of two points on a sphere. A

segment of a great circle is therefore the shortest path between two points located at locations (δ_1, λ_1) and (δ_2, λ_2) on a sphere.

To find the GCD, spherical coordinates have to be converted to Cartesian coordinates using Equation 2.1:

$$\boldsymbol{r_i} = a \begin{bmatrix} \cos\lambda_i \cos\delta_i \\ \sin\lambda_i \cos\delta_i \\ \sin\delta_i \end{bmatrix}, \tag{2.1}$$

where a is the radius of a sphere. Earth´s equatorial radius is approximately 6378 km while the mean radius is about 6371 km. Earth´s mean radius will be used in all calculations in this study. Moreover, latitude δ is related to the colatitude ϕ of spherical coordinates by $\delta = 90° - \phi$. The conversion to Cartesian coordinates therefore replaces $\sin\phi$ by $\cos\delta$ and $\cos\phi$ by $\sin\delta$. Figure 2.4 shows the spherical coordinates and the Cartesian coordinates in association with the Earth.

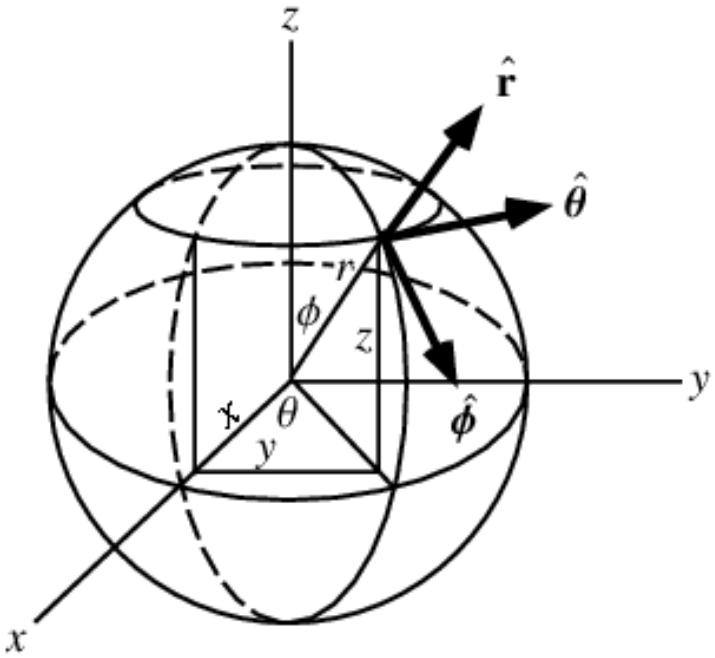

Figure 2.4: The spherical coordinates and cartesian coordinates in association with the Earth [28].

To find the angle α between two vectors $\mathbf{r_1}$ and $\mathbf{r_2}$ the dot product is used, see Equation 2.2:

$$\begin{aligned}\cos\alpha &= \boldsymbol{r}_1 \cdot \boldsymbol{r}_2 \\ &= \cos\delta_1 \cos\delta_2(\sin\lambda_1 \sin\lambda_2 + \cos\lambda_1 \cos\lambda_2) + \sin\delta_1 \sin\delta_2 \\ &= \cos\delta_1 \cos\delta_2 \cos(\lambda_1 - \lambda_2) + \sin\delta_1 \sin\delta_2.\end{aligned} \tag{2.2}$$

The GCD can then be found using Equation 2.3:

$$GCD = R\cos^{-1}[\cos\delta_1 \cos\delta_2 \cos(\lambda_1 - \lambda_2) + \sin\delta_1 \sin\delta_2], \tag{2.3}$$

where R is the mean radius of the Earth, which equals 6371 km.

2.6 The Relationship between True Airspeed and Ground Speed

Wind is basically an air mass moving in a definite direction over the surface of the Earth [29]. Therefore, if the wind is blowing from the east at 30 knots, it means that air is moving westward at the rate of 30 NM in one hour over the surface of the Earth. Obviously, an airplane flying within the moving mass of air will be affected (carried) by the wind. Therefore its motion over the surface of the Earth is a combination of two independent motion vectors that determine the position of an aircraft, i.e. the forward movement of the airplane through the air mass and the movement of the air mass relative to the surface of the Earth. True airspeed (TAS), which is the speed at which an aircraft moves through the air mass is determined by the pilot as well as the direction of movement referred to as heading. Ground speed and course, which are the horizontal speed of an aircraft and the direction of the velocity vector with reference to the ground, are however affected by wind vector. If an aircraft is flying in still air, the TAS and the GS will be the same and the aircraft´s ground track will be the same as the heading. However, this condition rarely exists. If an intended path of an aircraft is to the east, with a wind blowing from northeast, the heading of the aircraft must be somewhat to the north of east to offset drift. This is explained in the wind triangle in Figure 2.5. The long dotted line shows the direction the plane is heading, and the length of the line represents the airspeed for 1 hour. The short dotted line at the right shows the wind direction, and the length of the line represents the wind velocity for 1 hour. The solid line shows the direction of the track of the airplane as measured over the Earth, and the length

of the line represents the distance traveled in 1 hour, or the GS. As can be seen in the figure, the GS is less than the airspeed as the GS is affected by the wind.

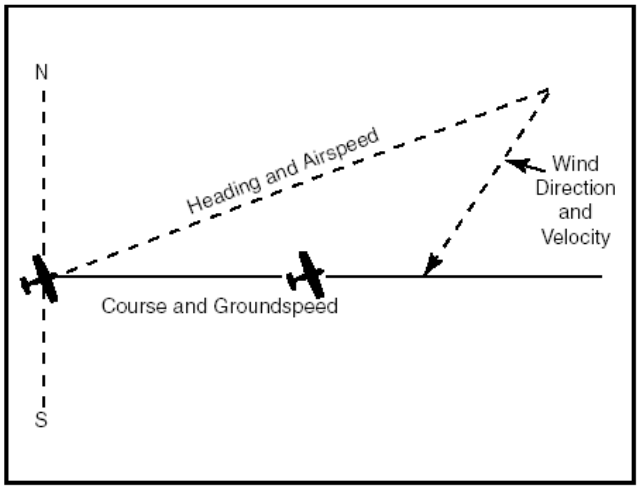

Figure 2.5: Wind triangle [29].

TAS and GS are essential elements in the WO model. In order to calculate GS, TAS is needed [30]. TAS is either calculated directly or indirectly in terms of Mach speed. The following relationship exists between TAS and Mach speed:

$$TAS = a_0 M \sqrt{\frac{T}{T_0}}, \tag{2.4}$$

where M is the Mach speed, a_0 is the speed of sound at standard sea level, T is static temperature in Kelvin degrees and T_0 is temperature at sea level under ISA conditions, which equals 288.15 Kelvin degrees. ISA decreases at a rate of about 2°C per 1,000 feet of altitude gain, so the static temperature at a regular cruising altitude of 36,000 feet would be around 216.15 Kelvin degrees[31].

The GS can be calculated from the time required to fly between two points with a known distance between them. In this study the GS can therefore be calculated by using the flight data received from Isavia as the data contain both time and distance between waypoints. If the aircraft heading is known the GS can also be determined by the vector sum of aircraft´s airspeed and heading, and the wind speed and direction, as explained by the wind triangle [29] in Figure 2.5. However in this current study the heading is not known. The GS is therefore calculated as TAS times the cosine of the Wind Correction Angle (WCA), plus the wind speed times the cosine of the Wind to Track Angle (WTAngle) [32].

$$GS = TAS \cdot \cos\,(WCA) + windspeed \cdot \cos\,(WTAngle), \tag{2.5}$$

where WCA is the correction applied to the course to establish a heading so that the track will coincide with the course and WTAngle is the difference between the wind direction and the track.

Chapter 3

The Data

When performing a study like this real world data from multiple sources is needed. It is important to get reliable flight data and accurate weather data as the results have to be very accurate. This research was done in collaboration with Isavia which provided all the flight data and IMR which provided all the weather data. In this chapter the weather data and the flight data will be represented along with the flights chosen for this optimization.

3.1 The Flight Data

Isavia provided a data set containing all the flight data needed. The data set was received in January 2014. The data contains information of all flights within the BIRD in the year 2011 throughout 2013. For each flight, information about aircraft operator, aircraft type, departure airport, arrival airport, total distance, total time, Mach speed, the planned route and the actual route are provided, among other. The planned route is the route that the aircraft plan beforehand and contains all waypoints from departure to arrival. For the planned route the waypoints are either given in waypoints that have a name or geographical waypoints. Named waypoints appear on aviation charts with known latitude and longitude. Examples of named waypoints are GUNPA and PEPKI. Geographical waypoint is a temporary position of an aircraft used in a planned route in areas where there are no named waypoints. Isavia, as most oceanic ATC, require the geographical waypoints to have latitudes and longitudes of whole numbers of degrees. The data for the route the aircraft actually flew are very accurate. It contains all the geographical waypoints the aircraft flew within the BIRD and sometimes several waypoints before the entry waypoint and after the exit waypoint. There is also accurate information about the time, distance to next waypoint, altitude, level change and Mach speed at each waypoint.

3.2 The Weather Data

The weather data was obtained from the IMR, the weather data is actual weather that was collected and post processed, in March 2014. The weather data obtained was for the three flights originally decided to optimize in order to achieve the most fuel efficiency. All these three flights flew from east to west. For all the three flights the North Atlantic jet stream was prevailing in the area of the actual flight plan. It was therefore considered beforehand that a significant fuel saving could be reached by minimizing the impact of the headwind for these flights, that is by choosing more wind optimal routes. The three days chosen were 28th of February 2013, 9th of October 2013 and 29th of November 2013. The time span for each set of weather data was 72-78 hours, spanning from 00:00 hours GMT on the 26th of February 2013 to 00:00 on the 1st of March 2013, from 00:00 hours GMT on the 7th October 2013 to 00:00 on the 10th October 2013 and from 00:00 hours GMT on the 27th November 2013 to 06:00 on the 30th November 2013. The weather data was received in Network Common Data Form (netCDF) format and was collected and post processed in March 2014. These data sets were defined on a grid with a 9 kilometer resolution in a horizontal plane in the altitudes of the flights chosen, which were 32,000 and 36,000 feet. The data set contained the following variables: height, time, longitude, latitude, wind direction, wind speed and temperature. The time is given with a 10 minute interval, the height is given in meters, the wind direction is given in degrees, the wind speed is given in meters per second and the temperature is given in Celsius degrees.

Furthermore new weather data sets were obtained in April 2014. These data sets contained the same information but were defined on a grid with a 9 kilometer resolution in horizontal plane in altitudes 1,000 feet above and below the cruising altitudes of the flights previously chosen, which were 32,000 and 36,000 feet. So, for 28th of February 2013 the new data set contained the same information but in the altitude of 31,000 feet and 33,000 feet. For 9th of October 2013 and 29th of November 2013 the new data sets contained the same information as the old ones except in the altitude of 35,000 and 37,000 feet. These data sets were obtained in the purpose to see if change in altitude would result in different optimization results.

3.3 Flights chosen for Optimization

As a starting point it was decided to find flights where it was considered a good chance that a high improvement in time could be reached. This was done by using National Oceanic and Atmospheric Administration´s (NOAA) website to find several days in 2013 where there were strong winds. Initially eight days were chosen where the jet stream effects were prevailing in BIRD. The flights on these eight days that had a significant difference between the planned flight time and the actual flight time were chosen for close examination. Finally three flights were chosen for optimization, where there was a difference of 13 to 17 minutes between the planned flight time and the actual flight time.

The first flight chosen was PIA781 on 29th of November 2013. The aircraft operator is Pakistan International Airlines Corporation, an aircraft type of Boeing 777-200LR, traveling from Benazir Bhutto International Airport to Toronto Pearson International Airport. The reason for choosing this flight beside from a delay of close to 17 minutes was that 11 waypoints were given in the actual flight plan whereas some of the flights had only 2 to 4 waypoints given in the actual flight plan. Figure 3.1 shows the mean jet stream effect at 34,000 feet on 29th of November 2013. The wind speed is given in m/s and ranges from under 10 m/s up to over 70m/s.

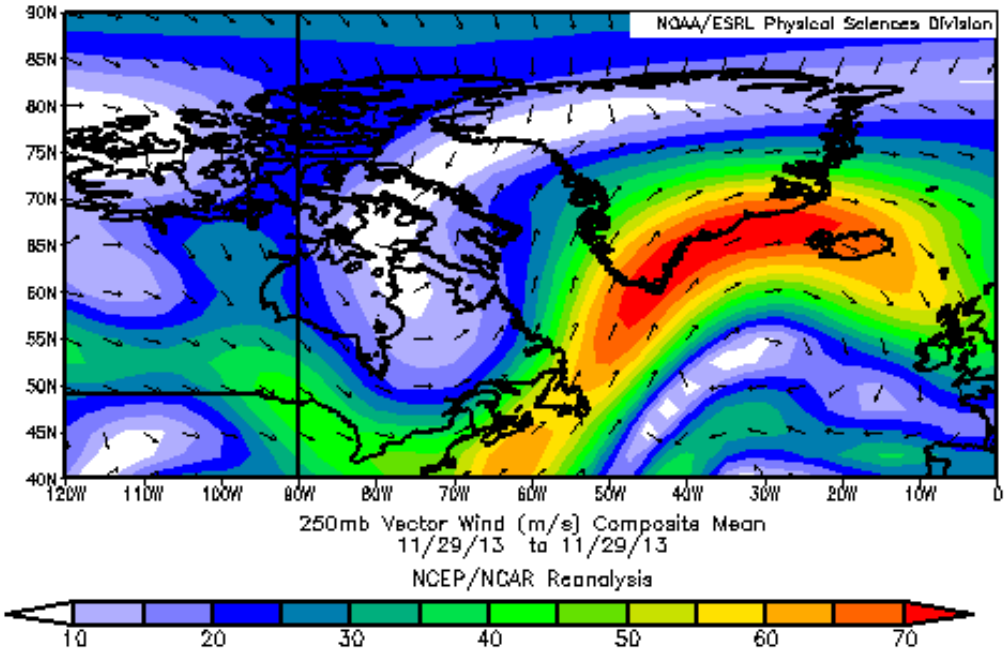

Figure 3.1: The mean vector wind in meters per second at 34,000 feet on 29th of November 2013 [12].

The second flight chosen was AFR084 on 28th of February 2013, the aircraft operator is Air France, an aircraft type of Boeing 777-200 traveling from Charles De Gaulle Airport to San Francisco International Airport with a delay of just over 13 minutes. The last flight chosen was AAL199 on 9th of October 2013, the aircraft operator is American Airlines Inc, an aircraft type of 767-300 traveling from Milano Malpensa Airport to John F. Kennedy International Airport with more than 16 minutes delay.

Furthermore, twelve more flights were chosen for optimization on 29th of November 2013 as the wind speed and the variation in the wind speed were high in the area where the grid was constructed that day. These flights will be presented in Chapter 6.5.

Chapter 4

The Wind Optimization Model

The purpose of the WO model is to find the shortest path with respect to time at a constant altitude in the cruise phase. Similar methodology is used in this current study as in the Cross-Polar Aircraft Trajectory Optimization and the Potential Climate Impact research study undertaken by NASA Ames Research Center [15]. An optimization algorithm is generated that finds wind optimal aircraft tracks that minimize aircraft fuel consumption by deviating from planned routes in the aim of reducing fuel burn. The aircraft course is therefore adjusted at each waypoint during cruise phase by changing aircraft heading. To be able to achieve this a WO model was constructed. The WO model takes flight data and weather data as input and produces the output, which is the minimum traveling time. There are many ways to construct a WO model, the method used in this current study will by described in this chapter.

4.1 Construction of the Grid

One way to perform the optimization and find the shortest path with respect to time is by constructing a grid around the actual flight track, which is used to deviate from the that track. The actual flight track is represented by geographical waypoints, where each waypoint is given in latitude and longitude. Latitude and longitude are two angles that specify the position of a point on the surface of the Earth [33]. They can both be represented in degrees and radians but in the flight data received from Isavia these geographical waypoints are always given in degrees. The angle between the plane of the equator and the line connecting the geographical waypoint in question to the Earth´s rotational axis is the latitude. In the northern hemisphere latitude is positive but in the southern hemisphere it is negative, ranging from -90° to + 90°. The angle at the center of the Earth between two planes which align with and intersect along the axis of rotation, orthogonal to the plane of the equator is the longitude and typically ranges from -180° to + 180°. In the WO model, each waypoint of the grid constructed is called a node and the distance between two waypoints is called a leg.

There are multiple ways to define the grid. One way, which was initially considered, is to construct a grid around the actual flight track by creating k times an off-set of $\pm$ 1 degree in

longitude and latitude, from the actual flight track. However, the route that an aircraft flies is never a straight line because on a surface of a sphere there are no straight lines. The shortest path between two points along the surface of the Earth is the great circle. Therefore it was concluded that a practical way to construct the grid around the flight track is by finding coordinates that are perpendicular to the actual coordinates. Also it was decided to define smaller separation between waypoints where needed.

The GCD between two waypoints given in the flight data can be up to several hundred NM. It can therefore be practical to add some waypoints in order to define smaller separation between the original waypoints, so more accuracy can be reached in the optimization. In this current study waypoints were added halfway between the original waypoints where the GCD between the two original waypoints was longer than 100 NM. Figure 4.1 shows the actual flight track for the flight PIA781 on 29th of November 2013, after the additional waypoints have been added. The waypoints shown in black represent the original waypoints while the waypoints shown in red represent the additional waypoints that have been added

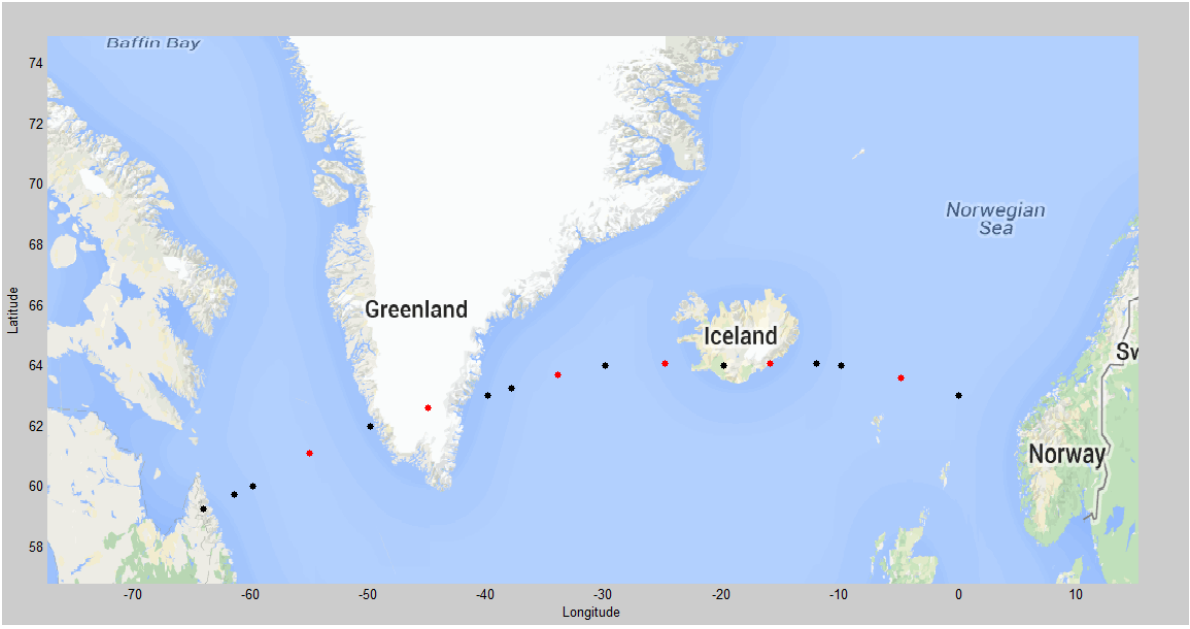

Figure 4.1: The actual flight track for the flight PIA781 on 29th of November 2013. The black waypoints are the original waypoints and the red waypoints are the waypoints that have been added where the GCD between the original waypoints was longer than 100 NM.

The next step is to construct the grid around the flight track where new waypoints are generated by computing coordinates that are perpendicular to the coordinates of the actual flight track. In this study a direction vector was constructed for the flight track, which was then turned at right angles clockwise to produce a perpendicular direction to the right. The

coordinates that are perpendicular to the coordinates of the actual flight track were calculated by moving k times $\pm \Delta$ degrees along the direction vector from the waypoints of the actual flight track. The Δ can be changed to any number, and can therefore be adapted in order to reach a maximum improvement. The number of waypoints generated by moving along the direction vector, defined as k, was chosen to be six in this current study but this number can however be changed to any number by a small alteration in the Matlab code. Figure 4.2 shows the grid constructed around the actual flight track for the flight PIA781 on the 29th of November 2013. The waypoints shown in black represent the actual flight track, after the additional waypoints have been added. The waypoints around the actual flight track represent the waypoints in the grid generated by moving $\pm$ 0.5, 1, 1.5, 2, 2.5, 3 degrees along the direction vector from the waypoints of the actual flight track.

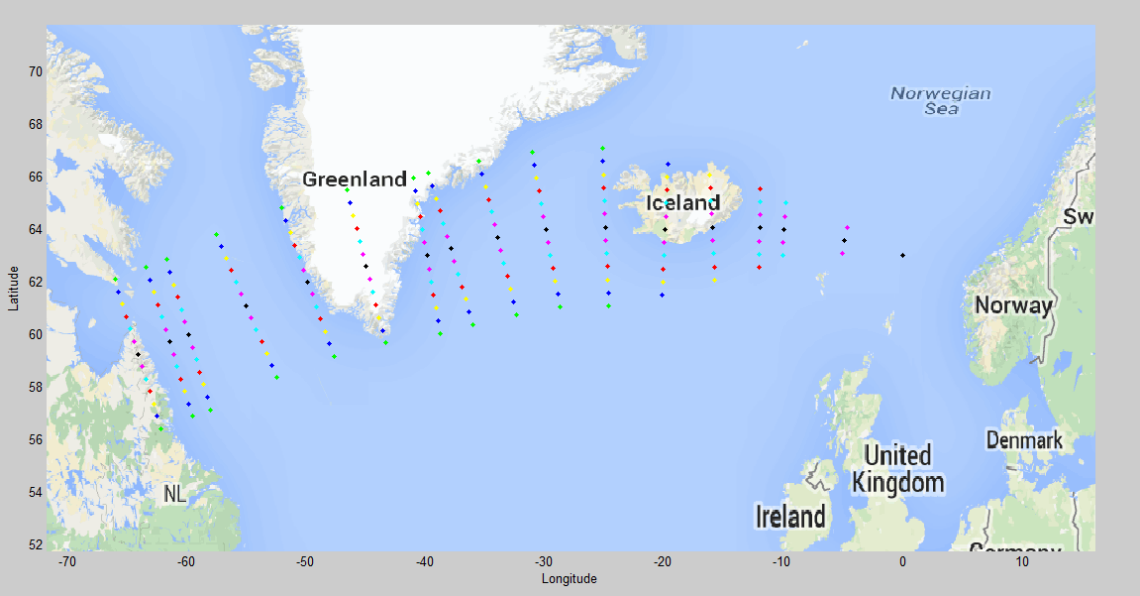

Figure 4.2: The grid generated around the actual flight track for the flight PIA781 on the 29th of November 2013.

The grid and the optimization model as a whole was constructed in that way that it can be used to optimize any flight, in spite of how many waypoints the actual flight track has. Furthermore, the grid was constructed in that way that it is possible to select how long the distance between the waypoints should be.

4.2 The Adjacency Matrix

The grid constructed in this study has $k \times 2 + 1$ columns, one column that represents the actual flight track, along with $k \times 2$ columns that where added for the purpose of the optimization by moving *k* times $\pm \Delta$ degrees along the direction vector. Numbers of rows are equal to *N*, where *N* is the number of waypoints for each flight, after the additional waypoints have been added. However in the first row of the grid there is only one node, this node is in column $k + 1$, which is the column that represents the actual flight track. In the second row there are 3 nodes in columns $k, k + 1$ and $k + 2$ as there are only legs between the first node to adjacent nodes. The empty nodes, which do not have any adjacent nodes are defined as not a number. In rows $k + 1$ to *N*, there are always $k \times 2 + 1$ nodes. This is explained better in Figure 4.3, where a directed graph is presented that has *k* equal to 6 and *N* equal to 17, the number of columns is therefore 13 and number of rows 17. The graph demonstrates which nodes are adjacent to which other nodes for the flight PIA781 on the 29th of November 2013. The adjacency matrix used in this study is the size of: $(N \times 13) - \sum_{n=1}^{6} 2n$, so if number of waypoints are 17 the adjacency matrix is the size of: $(17 \times 13) - \sum_{n=1}^{6} 2n$ = 179, the same size as in Figure 4.3.

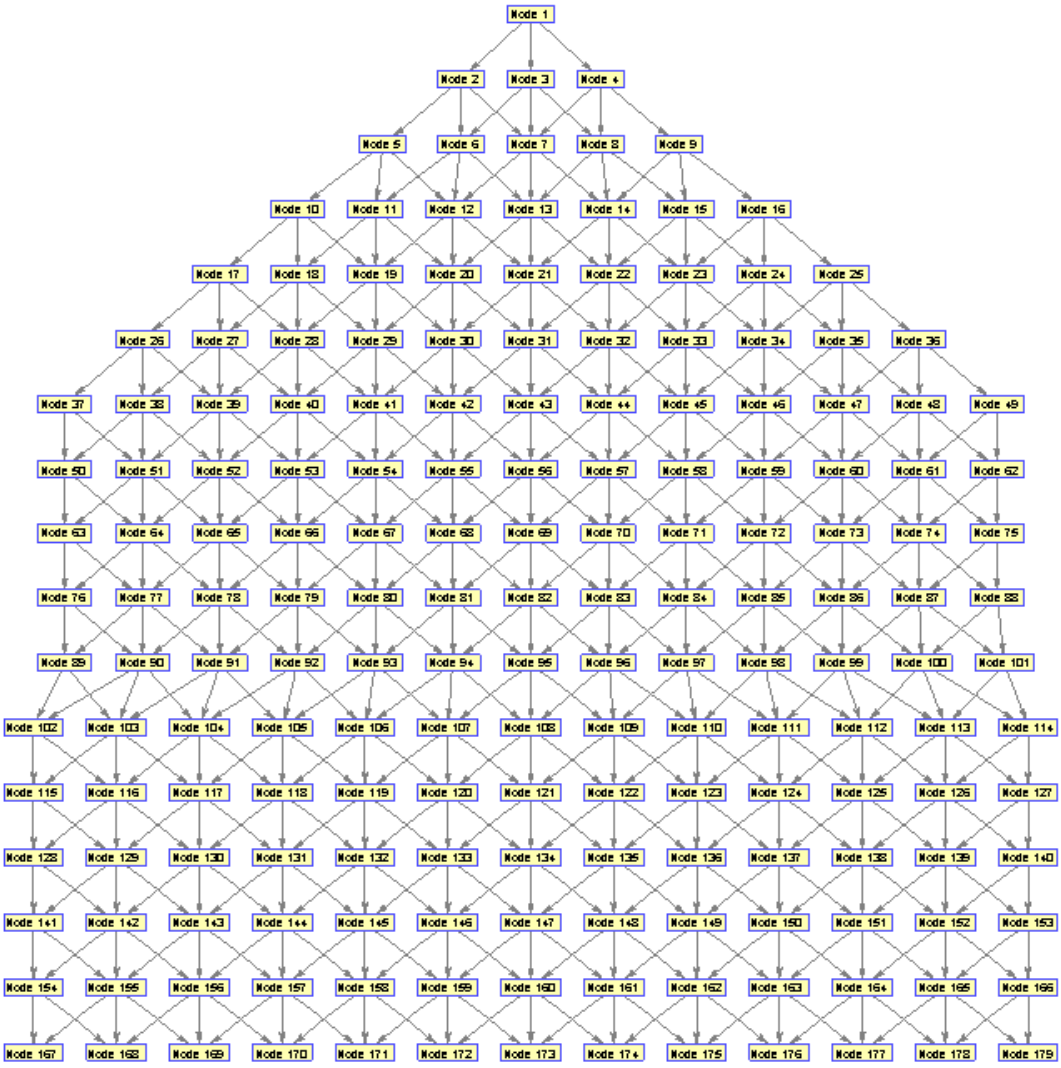

Figure 4.3: Directed graph that represents which nodes are adjacent for the flight PIA781 on 29th of November 2013.

4.3 The Development of the Wind Optimization Model

This study deals with wind optimization in the lateral plan at a constant cruise altitude, which is somewhat a simplification as aircrafts occasionally increase or decrease their altitude in the cruise phase. The lateral aircraft track is optimized by determining a heading angle that minimizes the objective function [15]. In order to find the optimal heading angle, with respect to wind, at a constant altitude *h* above Earth´s spherical surface, the following equations are needed:

$$\phi = \frac{V\cos\psi + u(\phi,\theta,h)}{R\cos\theta}, \tag{4.1}$$

$$\theta = \frac{V\sin\psi + v(\phi,\theta,h)}{R}, \tag{4.2}$$

$$\psi = \frac{-[F_w(\psi,\phi,\theta,u,v) + F_c(\psi,\phi,\theta,u,v,K)]}{R\cos\theta(C_t + K(\phi,\theta,h))}, \tag{4.3}$$

where ϕ is the longitude, θ is the latitude, ψ is the heading angle and V is the airspeed. $u(\phi,\theta,h)$ and $v(\phi,\theta,h)$ are the east-component of the wind velocity and the north-component of the wind velocity, respectively. $F_w(\psi,\phi,\theta,u,v)$ and $F_c(\psi,\phi,\theta,u,v,K)$ are aircraft heading dynamics in response to wind speed, wind direction and temperature. Finally, R is Earth´s radius, where it is assumed that the Earth is a square and R >> h. By integrating Equations 4.1, 4.2 and 4.3 using the initial aircraft position and the optimal heading, the optimal track in the presence of winds can be obtained.

The objective function is a cost function and contains components that penalize traveling time, these components are the wind speed, wind direction, temperature and GCD for each edge between all adjacent nodes in the grid constructed. The objective function is defined as:

$$J(h) = \int_{t_0}^{t_f} c_t\, dt, \tag{4.4}$$

where c_t is the cost coefficient of time and time is defined as the GCD divided with the GS. In this study the effect of vertical wind components on the aircraft are ignored as it would have increased the complexity of all calculations.

4.4 The Computations in Matlab

All calculations in this study were performed by Intel Core i7, 12 GB 1600 MHz DDR3 Toshiba Satellite S55-A5295 laptop. Matlab R2014a was used for all calculations and the algorithm. Matlab was also used to import, read and return the value of all the variables stored in the netCDF data files. Matlab contains all kinds of toolboxes that contain support functions that make complicated calculations easier. The Mapping toolbox contains number of navigational support functions. Two of these functions were used, one called *legs* and the other called *driftcorr*. The function *graphshortestpath* in the Bioinformatics toolbox in Matlab

was used for running the algorithm. These Matlab functions made the calculations much simpler and easier to work with.

4.5 The BADA Fuel Consumption Model

The Matlab toolbox Isavia provided containing all the flight data, also contains the Base of Aircraft Data (BADA) fuel consumption model. BADA is an Aircraft Performance Model (APM), which is developed and maintained by EUROCONTROL through effective collaboration with operating airlines and aircraft manufactures [23].

The fuel consumption model in Eurocontrol´s Base of Aircraft Data Revision 3.10 is used to compute fuel burn for aircraft cruise phase. The calculations are dependent on altitude, aircraft type, aircraft mass in kilograms, speed in terms of Mach number, temperature and which phase the aircraft is in, that is climb, cruise or descent phase. The BADA fuel consumption model is used to calculate the amount of fuel consumption in kg/min. After finding the amount of aircraft fuel consumption per minute, the amount of fuel saved by performing the optimization can be calculated. This is done by finding the amount of time saved in minutes by flying the wind optimal route, and multiplying the time saved with the aircraft fuel consumption per minute.

The BADA model uses the deviation from the temperature at sea level under ISA conditions, which equals to 288.15 K, to calculate the temperature at the altitude the aircraft is flying. However, as the weather data received from IMR only contains information about temperature at the flight level this has to be corrected. A modification was therefore made so the temperature at the flight level can be used instead of the temperature at sea level.

4.6 The Optimization Methodology

The following steps need to be performed in order to find the most efficient track for a flight in a cruise phase:

1. Define a smaller separation between waypoints of the flight track so more accuracy can be reached in the optimization. This is done by adding a waypoint halfway between the original waypoints where the GCD is longer than some distance *x*.

2. Now a matrix representing the grid around the actual flight track, after the additional waypoints have been added, has to be constructed. New waypoints are generated by computing coordinates that are perpendicular to the coordinates of the actual flight track. A direction vector is constructed for the flight track, which is then turned at right angles clockwise to produce a perpendicular direction to the right. The new coordinates that are perpendicular to the coordinates of the actual flight track are then calculated by moving k times $\pm\Delta$ degrees along the direction vector from the waypoints of the actual flight track. The matrix constructed has therefore $k \times 2 + 1$ columns, where column $k + 1$ represents the actual flight track and the other columns contain coordinates added for the purpose of the optimization. Numbers of rows are equal to *N*, where *N* is the number of waypoints for each flight, after the additional waypoints have been added. (The code used to construct the matrix that represents the grid is shown in Appendix A).

3. The next step is to calculate the GCD between every connected nodes of the grid. The GCD therefore has to be calculated from each node to all the adjacent nodes. These calculations result in a matrix of the size $(N - 1) \times (k \times 6 + 1)$. The middle column, which is column $k \times 3 + 1$, represents the GCD between all the waypoints of the actual flight track, after the additional waypoints have been added. Other columns of this matrix represent edges needed to cover all possible paths through the grid constructed. (The code used to construct the GCD matrix is shown in Appendix C).

4. Several software can be used to view the netCDF data files, containing the weather data. In this study the variables stored in the netCDF data files were imported into Matlab. The values of the variables were then read and returned.

5. A new matrix is constructed to find the mean wind speed and wind direction for each leg of the grid, constructed in step 2. This is done by constructing a new grid that is in the same resolution as the weather data, that is 9 km or around 5 NM between waypoints. The wind speed and wind direction at every point of the new grid is found.

This grid is then used to calculate the mean wind speed and wind direction for each leg of the grid constructed in step 2. This grid is also used to calculate the mean temperature in the area that the grid represents.

6. The next step is to calculate the GS. TAS, wind speed, wind direction and track angle are needed to calculate the GS. The wind speed and wind direction are calculated using the methodology in step 5. The track angle between every connected nodes of the grid is calculated, using the same methodology as in step 3, where the GCD between every connected nodes of the grid is calculated. The track angle calculations also result in a matrix of the size $(N-1) \times (k \times 6 + 1)$. The TAS is calculated using Equation 2.4, where TAS is equal to the speed of sound at standard sea level times the Mach speed times the square root of the static temperature divided by the mean temperature, calculated in step 5. (These calculations are shown in Appendix C).

7. Now the "cost" of each leg can be calculated. As the shortest path w.r.t. time is being calculated, the "cost" of each leg is the traveling time for that leg. The time, t_i, needed to travel leg i is therefore calculated as:

$$t_i = \frac{GCD_i}{GS_i}, \tag{4.5}$$

   Equation 4.5 represents the time needed to fly each leg. The time is dependent on the GCD of that leg and the GS of the aircraft while flying the leg.

8. Next, an adjacency matrix has to be constructed that specifies which nodes are connected to each other. (The code used to construct the adjacency matrix is shown in Appendix B).

9. At this point, when the time needed to travel each leg has been calculated and the adjacency matrix has been constructed, the next step is to run the Dijkstra´s algorithm. The algorithm is run for two cases. In the first case the exit point is fixed as the last waypoint of the actual flight track but in the latter case all exit points are allowed. The algorithm output consists of the shortest total time needed to traverse the grid, constructed in step 2, and the flight path that returns the shortest traveling time.

10. To estimate the fuel consumption per minute during cruise phase, the BADA fuel consumption model is used. The calculations are dependent on altitude, aircraft type, aircraft mass in kilograms, speed in terms of Mach number, temperature and which phase the aircraft is in, that is climb, cruise or descent phase. The altitude, aircraft type and the Mach speed are given the flight data received from Isavia. The mean temperature is calculated in step 5. The only unknown variable is the aircraft mass, this number is an approximation as the aircraft mass is not given in the flight data received from Isavia.

11. After finding the amount of aircraft fuel consumption per minute, the amount of fuel saved by performing the optimization can be calculated. This is done by finding the amount of time saved in minutes and multiplying the time saved with the aircraft fuel consumption per minute.

Chapter 5

Verification and Validation

Verification and validation are essential parts of this study. Many errors can occur in the development of computational models. It is therefore important to verify the models in this process. The WO model was verified in the development by testing all sub-models and the structures. Moreover, both the WO model itself and the data have to be validated to assure that the optimization results are in fact correct. The WO model can for example be validated by checking if the aircraft does deviate from the actual flight track when it should, that is when the weather conditions lead to shorter traveling time. When constructing a model, often some simplifications have to be made that affect the accuracy of the results. Therefore it is important to determine how accurate the WO model results are compared to reality. For the WO model, the accuracy can be tested by comparing the actual flight time to the flight time, calculated using the WO model. Furthermore, the data used in the running of the algorithm can contain some errors. When constructing a WO model, one of the most important factors that has to be validated is the weather data. The weather data used in this study was received from IMR, the weather data is actual weather that was collected and post processed and should therefore be accurate. However, it is essential that the weather data is validated to ensure that the optimization results are correct. In this chapter the WO model is validated, along with the weather data and the BADA model. Furthermore the accuracy of the WO model will be discussed.

5.1 Validating the Wind Optimization Model

The optimization model was validated by using artificial weather data. This was done to ensure that the optimization model works correctly. The aircraft should deviate from the actual flight track if it results in shorter flight time, when compared to the time it took to fly the actual flight track. When deviating from the actual flight track, the distance might be significantly longer than the distance of the actual flight track, therefore the weather condition have to be favorable in that way that the wind speed and wind direction lead to time savings although the distance flown might be longer.

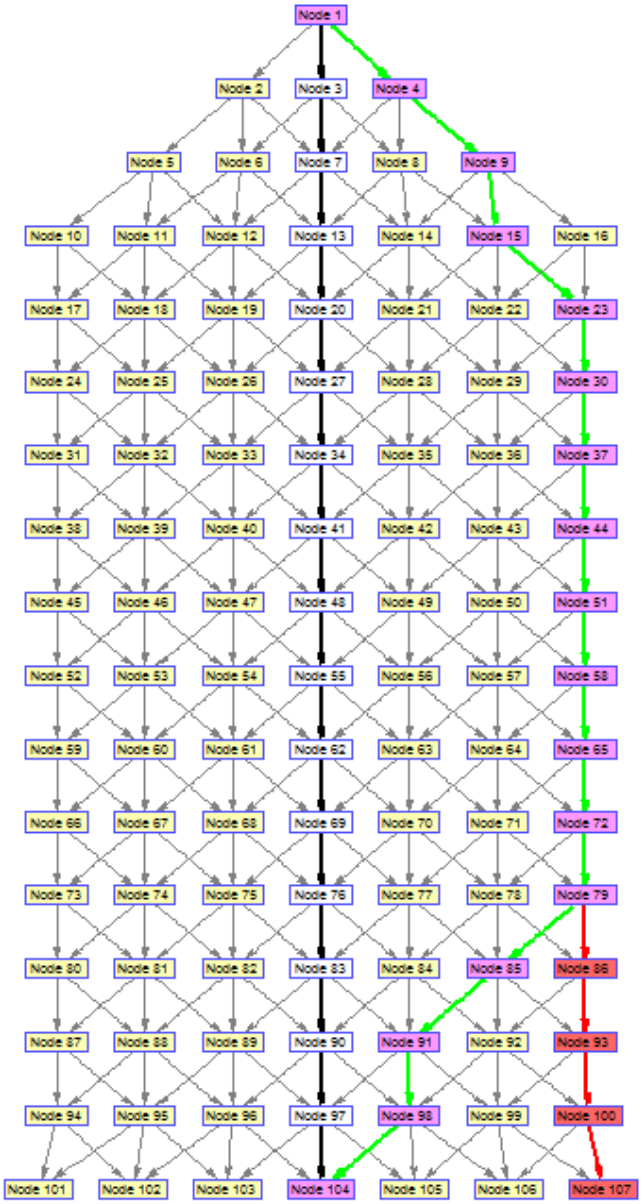

Figure 5.1: The shortest paths when the wind direction is 270° and the wind speed increases from south to north. The algorithm determines the southernmost flight track.

The WO model was validated using the flight PIA781 on the 29th of November 2013. The wind speed was first set to zero for the southernmost flight track and then increased to the north, the wind direction was set to 270 degrees, that is from west to east. As can be seen in Figure 5.1 the algorithm determines the southernmost flight track as the aircraft is flying from east to west and therefore it results in the smallest headwind. The black route in Figure 5.1 represents the actual route flown, the green route represents the shortest route in terms of time

if the exit point is fixed, that is the exit point has to be the last waypoint of the actual flight track. The red route represents the shortest route in terms of time if all exit points are allowed.

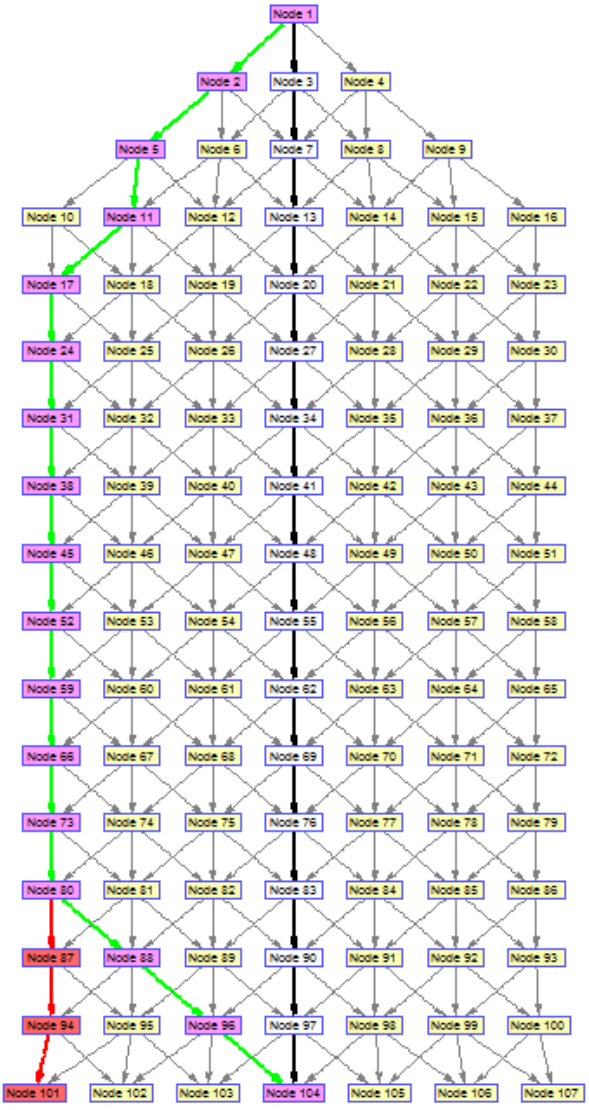

Figure 5.2: The shortest paths when the wind direction is 270° and the wind speed increases from north to south. The algorithm determines the northernmost flight track.

It was also decided to check if the opposite would happen if the wind speed would be set to zero for the northernmost flight track and then increased to the south. The wind direction was also set to 270 degrees for this validation. The results were as expected, in Figure 5.2 it can be seen that the algorithm determines the northernmost flight track as it results in the smallest headwind. The black route in Figure 5.2 represents the actual route flown, the green route represents the shortest route in terms of time if the exit point is fixed as the last waypoint of the actual flight track. The red route represents the shortest route in terms of time if all exit

points are allowed. These results indicate that the WO model works correctly as the algorithm determines the flight tracks that result in the smallest headwind and the shortest flight time.

5.2 Accuracy of the Wind Optimization Model

The accuracy of the WO model was tested by comparing the flight time calculated using the WO model to the actual flight time. Different types of grids can be constructed for the algorithm. These different types of grids affect the computational time and the accuracy in flight time. The accuracy of the WO model, using these different types of grids, was therefore compared to the computational time need to run the algorithm.

As there can be over 100 NM between adjacent waypoints in the grid used for the algorithm, the mean wind speed and wind direction for each leg of the grid were found instead of using the wind speed and wind direction closest to each waypoint. This was done by constructing a new grid where the distance between waypoints was decreased to the same resolution as the weather data, which is 9 km or approximately 5 NM. The new grid was then used to find the mean wind speed and wind direction for each leg of the original grid used for the algorithm. The mean wind speed and mean wind direction were calculated in order to obtain more accurate results.

Another approach is to construct a grid for the algorithm that has less distance between waypoints and uses the wind speed and wind direction closest to each waypoint. However this approach results in a big grid and consequently a large adjacency matrix. All the calculations and the running of the algorithm can therefore become slow. Nevertheless, this approach was used to test the improvements compared to the added computational time. It was decided to start by having the grid in the same resolution as the weather data, that is 9 km between each waypoint. This was too big for Matlab to handle as for example flight PIA781 on the 29th of November 2013 resulted in a grid and an adjacency matrix that has 16,844 nodes. However when the distance between points was increased to approximately 18 km or 10 NM, twice the resolution of the weather data, the algorithm found a result, in spite of a long computational time. In Table 5.1, comparison of the difference between actual total flight time for flight PIA781 and the total flight time computed by the WO model to the computational time needed to run the algorithm is provided. This comparison was done for a grid that has approximately 10, 20, 30 and 40 NM between waypoints and finally for the grid used in this

study which can have over 100 NM between waypoints but uses the mean wind speed and wind direction. As can be seen in Table 5.1 the grid that has 10 NM between waypoints results in the smallest error and which increases as the distance between waypoints is increased. However the grid used in this study, which can have over 100 NM between waypoints results in a smaller deviation than a grid which has around 40 NM between waypoints. The reason can be that the mean wind speed and wind direction are used in the former grid while the wind speed and wind direction closest to each waypoint is used in the latter one. Furthermore, there is a big difference in the computational time needed for the algorithm using the different types of grids. The highest computational time is 21 minutes and 57 seconds while the lowest computational time is 7 seconds. As can be seen in Table 5.1 there is a big difference in the computational time for a grid that has 10 NM between waypoints and the one that has 20 NM between waypoints, however there is a small difference in the error. The computational time decreases by 82.31% while the error only increases by 0.5%. Although the computational time decreases a lot from using a grid that has 10 NM between waypoints to using a grid that has 20 NM between waypoints, the computational time of 3 minutes and 53 seconds is still relatively high. By using the grid that can have over 100 NM between waypoints instead of using a grid that has 20 NM between waypoints, the error is increased by 0.23%. However the computational time is decreased down to 7 seconds or by 97.00%. Since it is much more convenient to work with the grid that can have over 100 NM between waypoints, as the computational time needed to perform the algorithm is only 7 seconds, this grid was used although the error is slightly higher.

Table 5.1: Comparison of the error between the actual flight time and the flight time calculated using the WO model and the computational time needed to perform the algorithm running for flight PIA781 on 29th of November 2013.

GCD between waypoints	Error	Number of nodes	Computational time
10 NM	1.00 %	5,984	00:21:57
20 NM	1.05 %	2,617	00:03:53
30 NM	1.23 %	1,507	00:01:32
40 NM	1.35 %	915	00:00:39
up to over 100 NM	1.28%	165	00:00:07

The difference between the actual flight time and the flight time calculated using the WO model is only around 1%, for all the approaches. A small error is common when constructing

a model like this as it is generally hard to get completely accurate results. The reason is that some simplifications often have to be made in the construction of the model that affect the accuracy of the model. Furthermore, a small error like this can possibly be caused by an error in the data used in the running of the algorithm. The accuracy of the data will be discussed in the next section.

5.3 Validating the Weather Data

The weather data can be validated in several ways. The preferred way would be to compare the weather data received from IMR to meteorological information derived from ADS-C messages [21]. As mentioned, specific ADS-C messages may contain meteorological information obtained from the flight management system. However the ADS-C messages only contain meteorological information when asked for. Before this study was conducted Reykjavik ACC did not ask for the meteorological information so they only received ADS-C message without the meteorological information. At the time the study was conducted Reykjavik ACC changed the content of their ADS-C messages and now the weather information is included. However, the implementation of this change was not finished before the submission of this study.

Another approach which can be used to validate the weather data is to compare the GS calculated using the flight data only to the GS calculated using the weather data. Since the flight data contain both time between waypoints and distance between waypoints the GS can be calculated by dividing the distance by the time. The GS can also be calculated using the weather data, along with the true airspeed and the heading of the aircraft, i.e. the air velocity vector. This is done by using Equation 2.5, where the GS is calculated as TAS times the cosine of the wind correction angle, plus the wind speed times the cosine of the wind to track angle. The results can be seen in Table 5.2. The difference between the mean GS calculated using flight data only and the mean GS calculated using the weather data ranged from 0.1% to 2.1% for all the fifteen flights that were considered in this study. This difference can partly be attributed to a possible error in the Mach speed as the Mach number is only given with two decimals. A change of $\pm$ 0.005 in Mach number results in significant change in GS. For the fifteen flights such change results in up to $\pm$ 0.9% change in GS. In the paper Analyses of the Speed Distribution of Aircraft that have an Assigned Mach Speed the speed distribution of

aircraft that have been assigned a fixed Mach speed in the Reykjavik CTA is analyzed [34]. The Mach speed that was obtained via ADC-reports was compared to the assigned Mach speed as issued in the North Atlantic region oceanic clearance. A total of 12,234 flights were examined, the results showed that there was a significant difference between the reported Mach speed in the ADS-C reports and the cleared Mach speed, where the standard deviation was 0.0042. These results verify that there is a significant inaccuracy in the Mach speed which consequently affects the GS. The difference between the GS calculated using the flight data only and the GS calculated using the weather data can therefore partly be explained by lack of accuracy in the Mach speed. In addition to this, some of the difference can be attributed to an error in the flight data as there can be up to a 2 NM offset to the right in the location of the actual waypoints compared to the reported waypoints. Some lack of accuracy in the GS calculated using the weather data can also be attributed to a long distance between each waypoint used in the algorithm running. Moreover, all distance calculations in the flight data assume that the Earth is a sphere instead of an ellipsoid but this simplification results in about 0.4% error which affects the GS calculated using the flight data. The results indicate that the weather data is accurate as the difference between the GS calculated using the flight data only and the GS calculated using the weather data is small for all the flights. The difference can probably be explained by a combination of all these different factors that have been mentioned. However the small difference in the GS subsequently affects the accuracy of the WO model, which will be discussed in Chapter 6.

Table 5.2: The difference between mean GS calculated using the flight data only and the mean GS calculated using weather data.

Flight	Mean GS calculated using flight data only (knots)	Mean GS calculated using weather data (knots)	Difference (%)
AFR084	459.1	460,7	+ 0.4
AAL199	405.2	402.6	– 0.6
PIA781	375.6	377.8	+ 0.6
UAE222	566.0	571.8	+ 1.0
KLM602	617.9	606.9	– 1.8
ELY032	581.1	570.7	– 1.8
AFL103	569.0	568.7	– 0.1
ANZ2	595.6	589.4	– 1.0
ACA850	559.2	551.3	– 1.4
BAW48	580.4	570.2	– 1.8
BAW84	563.3	554.3	– 1.6
FIN5	445.9	439.1	– 1.5
AIC191	429.4	438.4	+ 2.1
KLM602	549.4	541.5	– 1.4
DLH491	550.4	544.5	– 1.1

5.4 Validating the BADA Fuel Consumption Model

The results from the BADA fuel consumption model can be validated by comparing the calculated results to the BADA performance file which was included with the BADA fuel consumption model, received from Isavia. The BADA performance file presents the nominal fuel consumption per minute for all aircraft types, which are supported by the BADA revision, in a form of a look-up table [23]. The nominal fuel consumption per minute is presented for climb, cruise and descent phases for flight levels 0 to 430, where ISA temperature is used. However the fuel consumption per minute is only given at an interval of 2,000 feet. The fuel consumption per minute was not given for the cruising altitudes of the three flights that were originally chosen, which are 32,000 feet and 36,000 feet, but rather for 1,000 feet above and below these altitudes. It was therefore decided to validate the BADA

model using altitudes 1,000 feet below the cruising altitudes. The fuel consumption per minute in the BADA performance file is given for a specific Mach number that depends on the aircraft type and three mass levels that also depend on the aircraft type. The BADA fuel consumption model was used to calculate the fuel consumption per minute for each of the three aircraft types of the flights originally chosen. The Mach speed and the nominal mass level specified in the BADA performance file were used. The nominal mass level used in these calculations is the same as the mass used in the BADA fuel consumption calculations in this study. The nominal mass is 208,700 kg for aircraft type B772, 280,010 kg for aircraft type B77L and 154,590 kg for aircraft type B763. The Mach speed indicated in the BADA performance file is 0.84 for both the aircraft type B772 and B77L but 0.80 for aircraft type B763. The results from the BADA fuel consumption model were then used to validate the BADA fuel consumption model by comparing the results to the BADA performance file. The results are presented in Table 5.3. As can be seen from the table there is no difference between the fuel consumption per minute calculated using the BADA fuel consumption model and the fuel consumption per minute presented in the BADA performance file. It can therefore be concluded that the results from the BADA model are accurate.

Table 5.3: The difference between the fuel consumption per minute according to the BADA fuel consumption model and the BADA performance file.

Flight number	Aircraft type	Flight level	Fuel consumption per minute according to the BADA fuel consumption model (kg)	Fuel consumption per minute according to the BADA performance file (kg)
AFR084	B772	350	106.4	106.4
AAL199	B763	310	85.0	85.0
PIA781	B77L	350	128.1	128.1

Chapter 6

Results

The flights AFR084 on 28th of February 2013, AAL199 on 9th of October 2013 and PIA781 on 29th of November 2013 were chosen for two main reasons. The first reason is that the jet steam effects were prevailing in the BIRD on all of these dates. The second reason is that there was a significant difference between the planned flight time and the actual flight time for each of these flights. As can be seen in Table 6.1 this difference ranges from around 13 minutes up to nearly 17 minutes.

Table 6.1: The difference between the planned flight time and the actual flight time of flights AFR084, AAL199 and PIA781 chosen for optimization.

Flight number	Operator	Planned flight time	Actual flight time	Difference
AFR084	Air France	02:04:00	02:17:08	00:13:08
AAL199	American Airlines Inc.	01:44:00	02:00:33	00:16:22
PIA781	Pakistan International Airlines Corporation	04:32:00	04:48:53	00:16:53

When running the WO model it was realized that there was a small difference in the total flight time calculated by running the WO model for the actual flight track and the flight time given in the flight data received from Isavia. Table 6.2 shows the difference between the flight times calculated using the WO model and the flight times given in the flight data. As can be seen in Table 6.2, the difference is relatively small for these three flights; it ranges from 1.0% to 1.3%. It is generally hard to get completely accurate results from a model as there is usually some error in the data used or some simplification must be made in the model construction. The difference in the flight time can be attributed to some error in the flight data and the calculated GS. As mentioned above, the Mach number is only given with two decimals. A change of $\pm$ 0.005 in Mach speed results in up to $\pm$ 0.9% change in the GS. Furthermore, the flight data can contain a small error that can be caused by the offset to the right in the location of the waypoints, which can be up to 2 NM. A lack of accuracy in the calculated GS, which

can often be attributed to a long distance between each waypoint used in the algorithm running, can also lead to a small difference. Additionally, all distance calculations assume that the Earth is a sphere instead of an ellipsoid but this simplification results in about 0.4% error.

Although the difference is small the improvement expected by flying WO routes is only 1-2% so that numerical accuracy is a very important factor in this study. To get the most accurate results it was therefore decided to compare the shortest flight time calculated using the WO model to the flight time of the actual track, calculated by using the WO model.

Table 6.2: The difference between the total flight time calculated using the WO model and the total flight time given in the flight data received from Isavia.

Flight number	Operator	Total flight time given in the flight data (minutes)	Total flight time calculated using the WO model (minutes)	Difference (%)
AFR084	Air France	137.13	135.33	– 1.3
AAL199	American Airlines	120.70	121.93	+ 1.0
PIA781	Pakistan International Airlines	288.88	285.19	– 1.3

The shortest path was found for two types of constraints, for each of the three flights. In both cases the starting point was fixed as the first waypoint of the actual flight track. However, in the first case all exit points were allowed but in the second case the only exit point allowed was the last waypoint of the actual flight track. The first case was defined to find the maximum potential improvement that can be reached. However airlines cannot always choose the exit point as the exit point is often fixed by ATC because of requirements of the entry point into next ATC area. Furthermore, when all exit points are allowed the distance flown within the area which is being optimized can often be reduced significantly. Reduced distance in the area may however lead to a longer distance from the exit point to the arrival airport. Moreover, the total distance from entry point to arrival airport could also be longer, compared to the distance if the actual flight track had been flown. The improvement obtained when all exit points are allowed could therefore be misleading. However, this problem can be solved by adding the Great Circle Distance from the exit points to the arrival airport and thereby find the exit point that results in the most improvement from the entry point all the way to the arrival airport. However in this study the weather data were not available for the whole flight profile. Therefore artificial weather would have to be used, which could lead to inaccurate

results. The first case, where all the exit points are allowed will be calculated for all the three flights but the limitations on exit points will be discussed for each flight. The latter case, where the exit point is fixed, does however give a better representation of the improvement that is actually reachable.

6.1 The Flight PIA781 on 29th of November 2013

The first flight chosen for optimization was PIA781 on 29th of November 2013. The aircraft operator is Pakistan International Airlines, this is an aircraft type of Boeing 777-200LR, traveling from Benazir Bhutto International Airport to Toronto Pearson International Airport. The reason for choosing this flight, besides a difference of close to 17 minutes between the actual flight time and the planned flight time, was because the flight time given in the flight data was close to 5 hours and the number of waypoints was higher than for most flights. Although not all of the waypoints are within BIRD, it was still decided to use all available waypoints for the purpose of determining the improvement obtainable for the entire flight track provided by the flight data. The point referred to as exit point is therefore not the exit point of the BIRD area but rather the last waypoint of the actual flight track given by the flight data. Figure 6.1 shows the grid constructed around the actual flight track for flight PIA781.

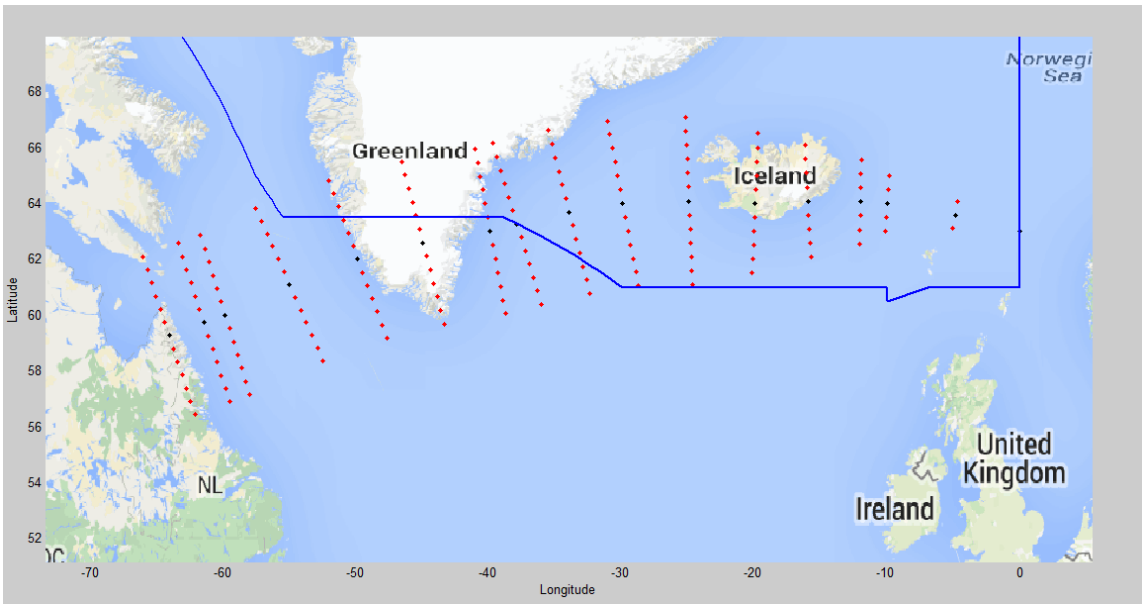

Figure 6.1: The grid generated around the actual flight track for the flight PIA781 on 29th of November 2013. The area within the blue line represents the Reykjavik CTA.

The waypoints shown in black represent the actual flight track, after the additional waypoints have been added. The area within the blue line represents Reykjavik CTA, as can be seen in the figure only the first 10 waypoints are within BIRD but the other waypoints are within the Gander FIR.

The algorithm found an optimal solution for both cases, which resulted in significant improvements from the total flight time of the actual track, calculated using the WO model. Figure 6.2 shows the deviation from the actual flight track, where the black path represents the actual track. The red path shows the shortest time-path if all exit points are allowed while the green path shows the shortest time-path if the exit point is fixed as the last waypoint of the actual flight track. The time needed to fly the actual flight path, calculated using the WO model was 285.2 minutes. The time needed to fly the red path, which is the shortest time-path if all exit points are allowed, was 272.3 minutes. This equals an improvement of 12.9 minutes or 4.5% in flight time. The time needed to fly the green path, which is the shortest time-path if the exit point is fixed as the last waypoint of the actual flight track, was however 280.5 minutes. This equals an improvement of 4.7 minutes or 1.6% in flight time.

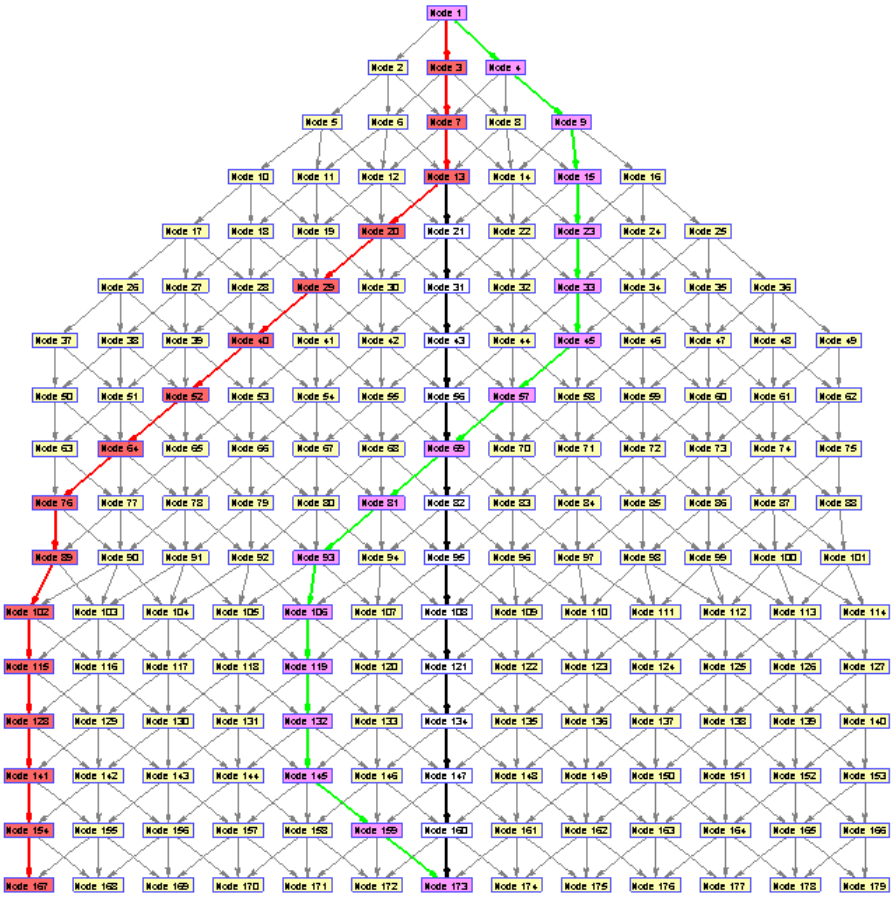

Figure 6.2: The shortest paths calculated using the optimization algorithm generated for the two cases for flight PIA781 on the 29th of November 2013.

The actual track flown was 1,808.4 NM in length. The red track, where all exit points were allowed, was however 1,764.3 NM in length or 44.2 NM shorter than the actual track. The red track was therefore 2.4% shorter than the actual track; however it took 4.5% less time to travel this track compared to the actual track. The green track, where the exit point was fixed as the last waypoint of the actual flight track, was 1,833.2 NM in length or 24.7 NM longer than the actual track. The green track was 1.4% longer than the actual track; however it took 1.6% less time to travel this track compared to the actual track. The difference between the red and the green tracks is that the green track has the extra constraint that the exit point must be the same as the last waypoint of the actual track. The green track is therefore usually longer than the red track and the wind can also be less favorable for the green track than the red track. However the high improvement reached for the case where all exit points are allowed gives a misleading conception. Although flying the red path leads to less headwind than flying the actual route, choosing this exit points leads to 10.1% longer distance from exit point to arrival airport, compared to the actual track. Moreover, choosing this exit point results in 2.3% longer total distance from entry point to arrival airport compared to the actual track. However, in spite of longer total distance this exit point could possibly have resulted in the shortest flight time but because of a lack of weather data it could not be verified.

Figure 6.3 shows the actual flight path compared to the shortest path in terms of time for the two cases. The black route shown in the figure represents the actual flight track, the red route represents the shortest path, if all exit points were allowed, and the green route represents the shortest path, if the exit point was fixed as the last waypoint of the actual flight track. The two cases result in very different paths although the green path has only one extra constraint. The red path is 3.8% shorter than the green path and results in 2.9% shorter flight time.

The BADA fuel consumption model is used to estimate fuel burn for the aircraft cruise phase. The calculations are dependent on altitude, aircraft type, aircraft mass in kilograms, speed in terms of Mach number, temperature and phase of flight, that is climb, cruise or descent phase. Information about altitude, aircraft type and Mach speed are found in the flight data received from Reykjavik ACC. The aircraft was flying at a cruising altitude of 36,000 feet (FL 360), the aircraft is of the type Boeing 777-200LR and the cruise speed in terms of Mach number was 0.83. As the aircraft mass is not given in the flight data the nominal weight for this type of aircraft, which is given in the BADA performance file, was used. The nominal weight for Boeing 777-200 is 280,010 kg.

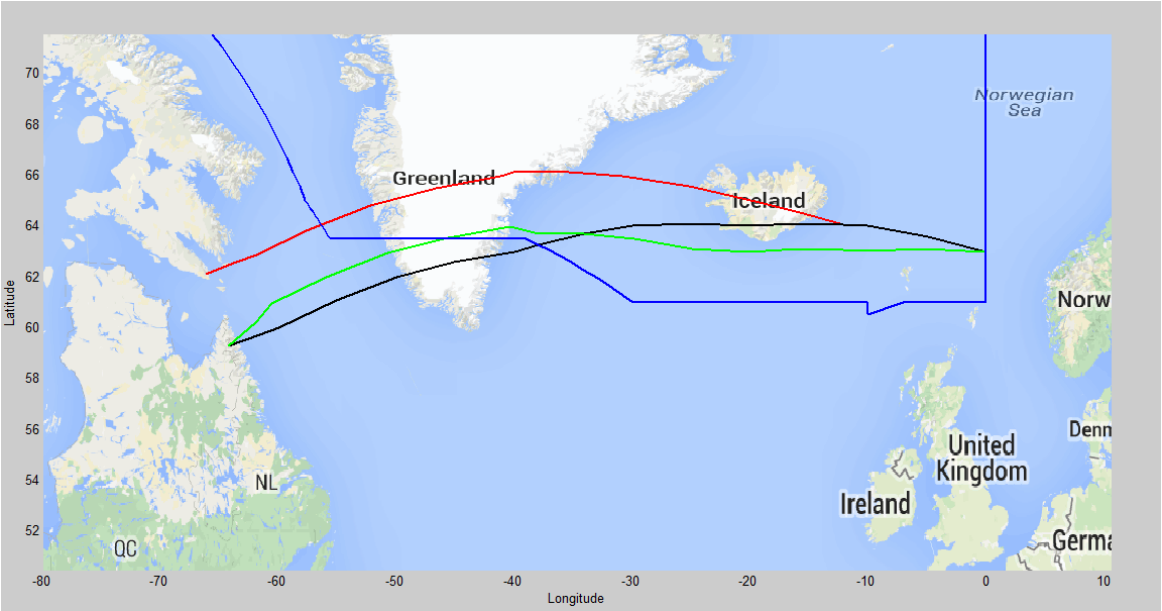

Figure 6.3: The actual flight path and the shortest paths calculated for both cases of flight PIA781. The actual flight path is shown in black, the shortest path if all exit points are allowed is shown in red and the shortest path if the exit point is fixed is shown in green. The area within the blue line represents the Reykjavik CTA.

The BADA model uses a deviation from the temperature at sea level under ISA conditions to calculate the temperature at the altitude that the aircraft is flying. However as the weather data received from IMR only contains information about temperature at each flight level this had to be corrected. A modification was therefore made so the temperature at the flight level could be used instead of the temperature at sea level. These parameters were put into the BADA fuel consumption model. Calculated aircraft fuel consumption per minute according to these parameters was 125.2 kg. According to these calculations the fuel saved was 581.8 kg when the exit point was fixed as the last waypoint of the actual flight track and 1,612.6 kg when all exit points were allowed. These calculations are however not accurate as the exact mass of the aircraft is not known and therefore had to be estimated. Furthermore, the mean temperature in the area of the grid constructed was used instead of using the mean temperature of each calculated track. The reason is that the difference between the mean temperature in the area where the grid was constructed and the mean temperature of each calculated track was very small and the effect it had on the fuel burn was insignificant. In addition to this, it was decided to check if there was a significant difference between the fuel consumption calculated using the mean temperature at each flight level and the temperature at sea level under ISA conditions. For the flights PIA781, AAL199 and AFR084 this only resulted in 0.16% to 0.31% change in fuel consumption. The effects are therefore minimal. However since the temperature at each flight level was given in the weather data, the mean temperature in the

area of the grid constructed was used in all calculations in order to obtain more accurate results. The optimization results for flight PIA781 are summarized in Table 6.3.

Table 6.3: Summary of the optimization results for flight PIA781.

Case	Improvement in flight time compared to the actual flight path (minutes)	Improvement in flight time compared to the actual flight path (%)	Fuel saved (kg)
Fixed exit point (green path)	4.7	1.6	581.8
All exit points allowed (red path)	12.9	4.5	1,612.6

The relatively high improvement reached for flight PIA781 can be the result of very high wind speed in the area and high variation of the wind speed, on this day. The mean wind speed in the area where the grid was constructed was 107.1 knots or 55.1 m/s. The wind speed standard deviation with respect to space was 14.0 knots or 7.2 m/s. The headwind was therefore very strong and as the wind speed standard deviation was relatively high deviating from the actual track resulted in significant improvement in flight time as the impact of headwind was minimized. Another factor that might affect the optimization result is that the aircraft had been flying from Pakistan and had been in air for over 7 hours when entering the BIRD. The weather forecast that was used could therefore be old. Also, it is not known what kind of optimization system the airline might be using when planning their routes.

6.2 The Flight AAL199 on 9th of October 2013

The second flight chosen for optimization was AAL199 on 9th of October 2013. The aircraft operator is American Airline and the aircraft type is Boeing 767-300, flying from Milano Malpensa Airport to John F. Kennedy International Airport. The reason for choosing this flight was that the jet steam effects were prevailing in BIRD on this date. Moreover, there was a significant difference between the planned flight time and the actual flight time, where the actual flight time was over 16 minutes longer than the planned flight time. Figure 6.4 shows the grid constructed around the actual flight track for the flight AAL199. The waypoints

shown in black represent the actual flight track, after the additional waypoints have been added.

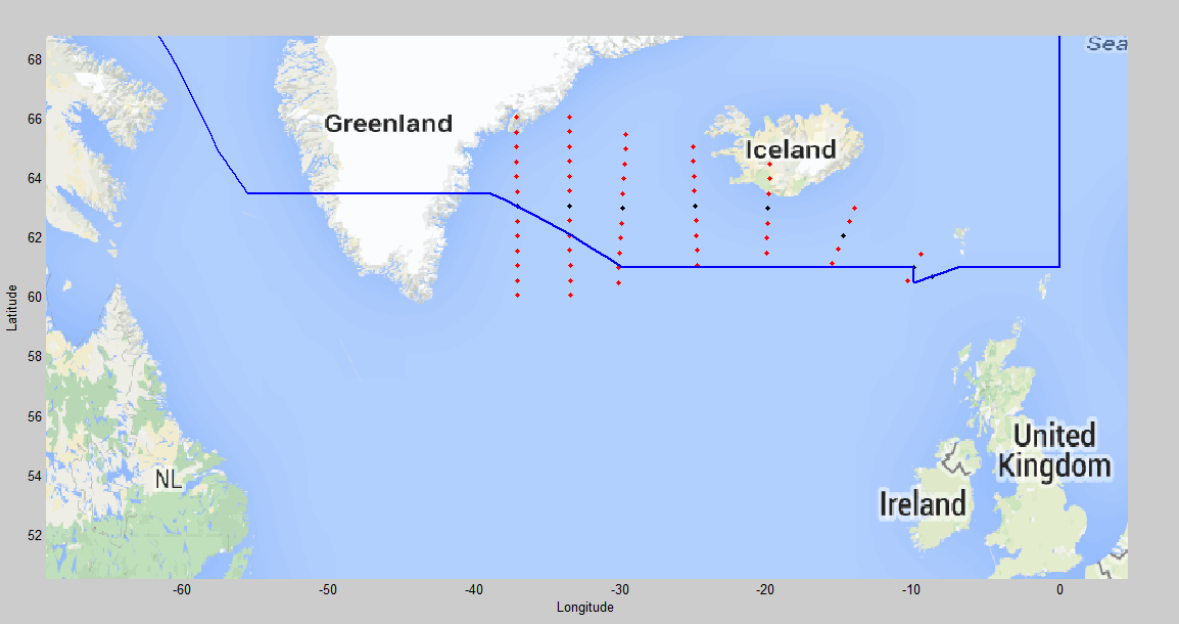

Figure 6.4: The grid generated around the actual flight track for the flight AAL199 on 9th of October 2013. The area within the blue line represents the Reykjavik CTA.

The algorithm found an optimal solution for both cases. Figure 6.5 shows the deviation from the actual flight track, where the black track represents the actual track. The red path shows the shortest time-path if all exit points are allowed while the green path shows the shortest time-path if the exit point is fixed as the last waypoint of the actual flight track.

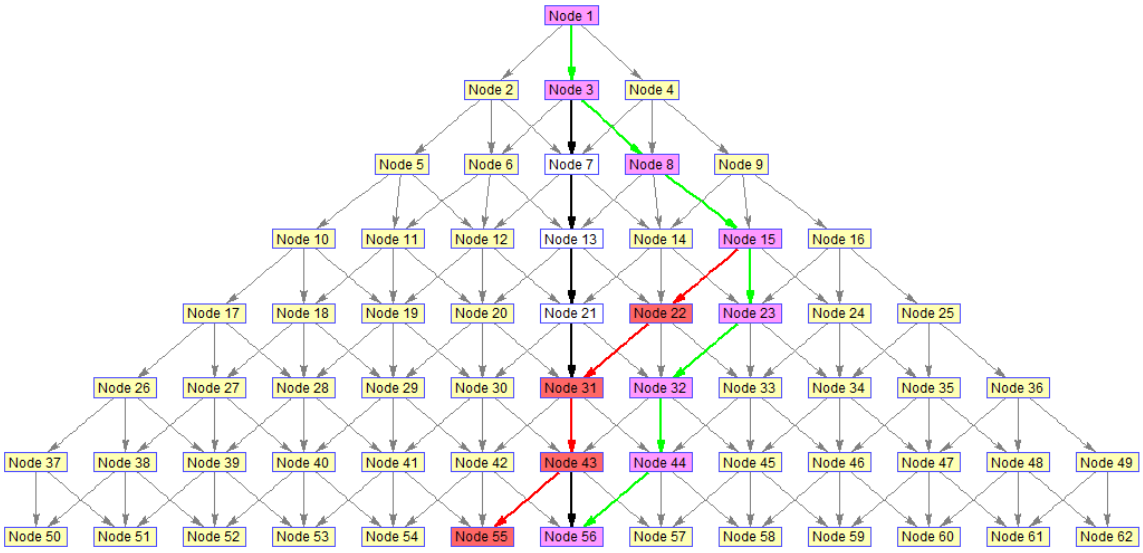

Figure 6.5: The shortest paths calculated using the optimization algorithm generated for the two cases for flight ALL199 on the 9th of October 2013.

The time needed to fly the actual flight path, calculated using the WO model, was 121.9 minutes. The time needed to fly the red path, which is the shortest path in terms of time if all exit points are allowed, was 120.7 minutes. This equals an improvement of 1.2 minutes or 1.0% in flight time. The time needed to fly the green path, which is the shortest time-path if the exit point is fixed as the last waypoint of the actual flight track, was also 120.7 minutes. This equals an improvement of 1.2 minutes or 1.0% in flight time.

The actual track flown was 814.1 NM in length. The red track, where all exit points were allowed, was however 815.3 NM in length or 1.2 NM longer than the actual track. The red track is therefore 0.1% longer than the actual track; however it took 1.0% less time to travel this track compared to the actual track. The green track, where the exit point is fixed as the last waypoint of the actual flight track, was 817.4 NM in length or 3.3 NM longer than the actual track. The green track is 0.4% longer than the actual track in terms of distance; however it took 1.0% less time to travel this track compared to the actual track. The green track is 0.3% longer than the red track but it took the same time to travel both of these tracks. Having the constraint that the exit point has to be the same as the last waypoint of the actual track does therefore not have any impact on the traveling time for flight AAL199. However the red path results in 0.8% longer distance from exit point to arrival airport when compared to the distance from the exit point of the actual flight track to arrival airport. When the total improvement from entry point to arrival airport is considered, the green path would therefore result in more improvement in flight time.

Figure 6.6 shows the actual flight path compared to the shortest paths calculated for the two cases. The black route shown in Figure 6.6 represents the actual flight track, the red route represents the shortest time-path, if all exit points are allowed, and the green route represents the shortest time-path, if the exit point is fixed as the last waypoint of the actual flight track. The green and the red tracks are identical for the first half of the route. The red track then deviates from the green track as it has not the same constraint as the green track, which is that the end waypoint is fixed as the last waypoint of the actual flight track. The red track therefore found a route that is 0.3% shorter than the green track, in terms of distance, but resulted in the same traveling time. However, as mentioned above these results are limited to this part of the flight only.

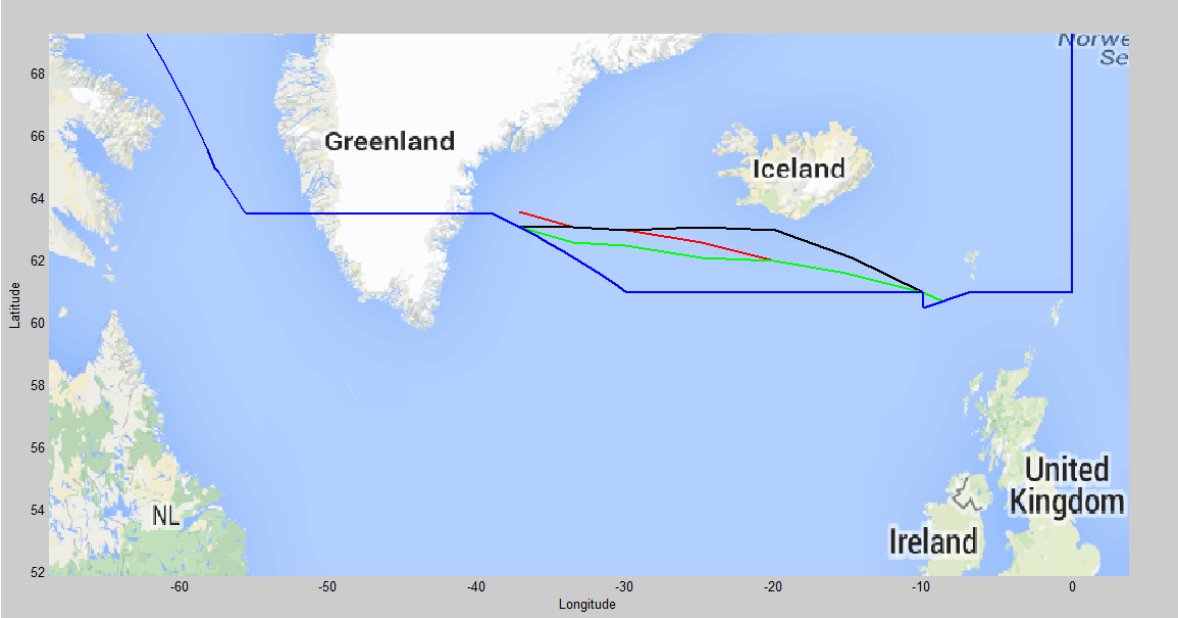

Figure 6.6: The actual flight path and the shortest paths calculated for both cases of flight AAL199. The actual flight path is shown in black, the shortest path if all exit points are allowed is shown in red and the shortest path if the exit point is fixed is shown in green. The area within the blue line represents the Reykjavik CTA.

The BADA fuel consumption model was used to estimate the fuel burn for the aircraft cruise phase. The aircraft was flying at a cruising altitude of 32,000 feet, the aircraft is of the type Boeing 767-300 and the cruise speed in terms of Mach number was 0.80. As the aircraft mass is not given in the flight data the nominal weight for this type of aircraft, which is given in the BADA performance file, was used. The nominal weight for Boeing 767-300 is 154,590 kg. These parameters, along with the mean temperature, were put into the BADA fuel consumption model. Calculated aircraft fuel consumption according to these parameters was 83.2 kg/min. According to these calculations the fuel saved was 100.3 kg when the exit point was fixed and 100.4 kg when all exit points were allowed. These calculations are however not accurate as the exact mass of the aircraft is not known and therefore has to be estimated. However they give a good indication of the potential fuel savings. The optimization results for flight AAL199 are summarized in Table 6.4.

The improvement reached in flight AAL199 can be attributed to relatively high wind speed in the area and high variation in wind speed. The mean wind speed in the area where the grid was constructed was 38.1 m/s. The wind speed standard deviation with respect to space was 6.9 m/s. The headwind was therefore strong and as the wind speed standard deviation was high, deviating from the actual track resulted in significant improvement in flight time as the impact of headwind was minimized.

Table 6.4: Summary of the optimization results for flight AAL199.

Case	Improvement in flight time compared to the actual flight path (minutes)	Improvement in flight time compared to the actual flight path (%)	Fuel saved (kg)
Fixed exit point (green path)	1.2	1.0	100.3
All exit points allowed (red path)	1.2	1.0	100.4

6.3 The Flight AFR084 on the 28th of February 2013

The last flight chosen for optimization was AFR084 on 28th of February 2013. The aircraft operator is Air France, this is an aircraft type of Boeing 777-200, flying from Charles de Gaulle Airport to San Francisco International Airport. The jet steam effects were prevailing in BIRD on this date but the wind speed was however not as strong as on the dates of the two flights previously considered. There was a significant difference between the planned flight time and the actual flight time, where the actual flight time was over 13 minutes longer than the planned flight time.

The waypoints around the actual flight track were first generated in the same way as for the other flights, that is by moving $\pm$ 0.5, 1, 1.5, 2, 2.5, 3 degrees along the direction vector from the waypoints of the actual flight track. As mentioned, the direction vector was constructed for the flight track and then turned at right angles clockwise to produce a perpendicular direction to the right. The new waypoints are therefore perpendicular to the waypoints of the actual track. However this grid resulted in the green track, which is the shortest time-path when the exit point was fixed as the last waypoint of the actual flight track, being the same as the actual flight track. The red track, which is the shortest time-path when all exit points were allowed, resulted in an improvement of 0.3% in flight time when compared to the actual track. Since the shortest time-path was the same as the actual path when the exit point was fixed it resulted in no improvement in flight time when compared to the actual flight time, calculated using the WO model. The reason for this is that although the jet stream effects were prevailing

in the area there was small variation in the wind speed. Therefore deviating from the actual track did not result in a shorter flight time, when the exit point was fixed. It was therefore decided to generate the grid by moving $\pm$ 0.25, 0.5, 0.75, 1, 1.25, 1.5 degrees along the direction vector from the waypoints of the actual flight track. By doing this, the extra distance needed to deviate from the actual flight track was decreased and therefore more likely to find new paths that resulted in shorter traveling time. Figure 6.7 shows the grid constructed around the actual flight track for flight AFR084. The waypoints shown in black represent the actual flight track, after the additional waypoints have been added.

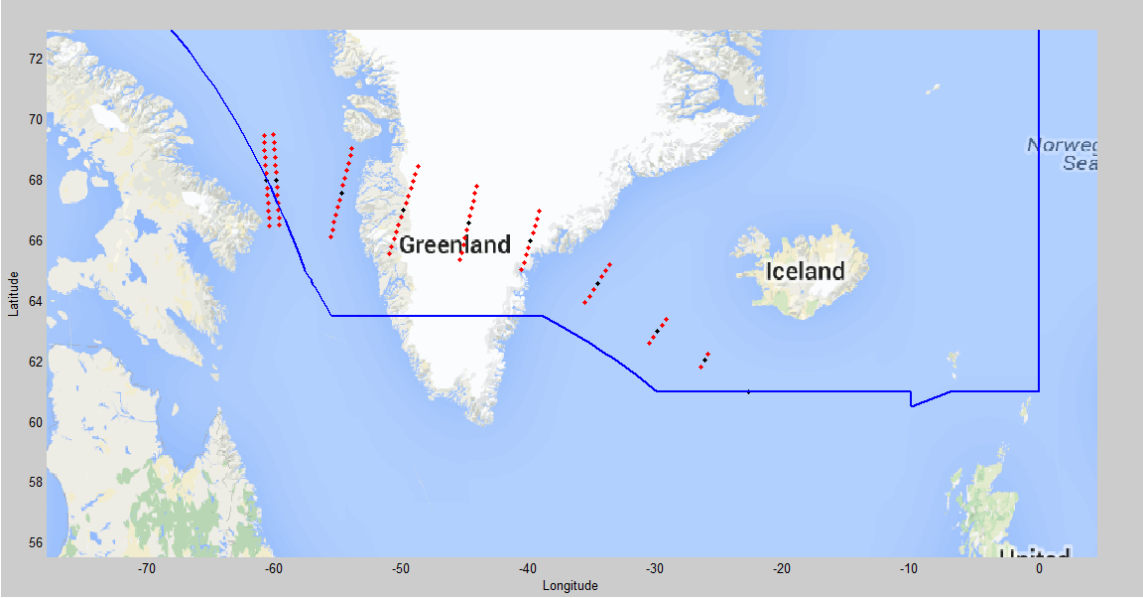

Figure 6.7: The grid generated around the actual flight track for flight AFR084 on the 28th of February 2013. The area within the blue line represents the Reykjavik CTA.

The algorithm found an optimal solution for both cases. Figure 6.8 shows the deviation from the actual flight track, where the black track represents the actual flight track. The red path shows the shortest time-path if all exit points are allowed while the green path shows the shortest time-path if the exit point is fixed as the last waypoint of the actual flight track. The flight time needed to fly the actual flight path, calculated using the WO model, was 135.3 minutes. The time needed to fly the red path, which was the shortest time-path if all exit points were allowed, was 134.8 minutes. This equals an improvement of 34 seconds or 0.4% in flight time. The time needed to fly the green path, which was the shortest time-path if the exit point was fixed as the last waypoint of the actual flight track, was however 135.0 minutes. This equals an improvement of 20 seconds or 0.2% in flight time. The improvement in flight time for flight AFR084 was therefore very small compared to the improvement

achieved for the other two flights. The reason is, as mentioned above, that although the jet stream effects were prevailing in the area there was a small variation in the wind speed. The mean wind speed in the area where the grid constructed was 27.0 m/s. The wind speed standard deviation in terms of space was however only 2.0 m/s, which is low compared to the other two flights. Although the headwind was relatively strong, the wind speed standard deviation was low. Deviating from the actual track did therefore not result in very low improvement in flight time. However changing the grid resulted in a higher improvement compared to that achieved using the prior grid. Using the prior grid resulted in no improvement in flight time when the exit point was fixed while using this grid resulted in an improvement of 0.2%. The improvement when all exit points were allowed increased from 0.3% to 0.4% or by 0.1%

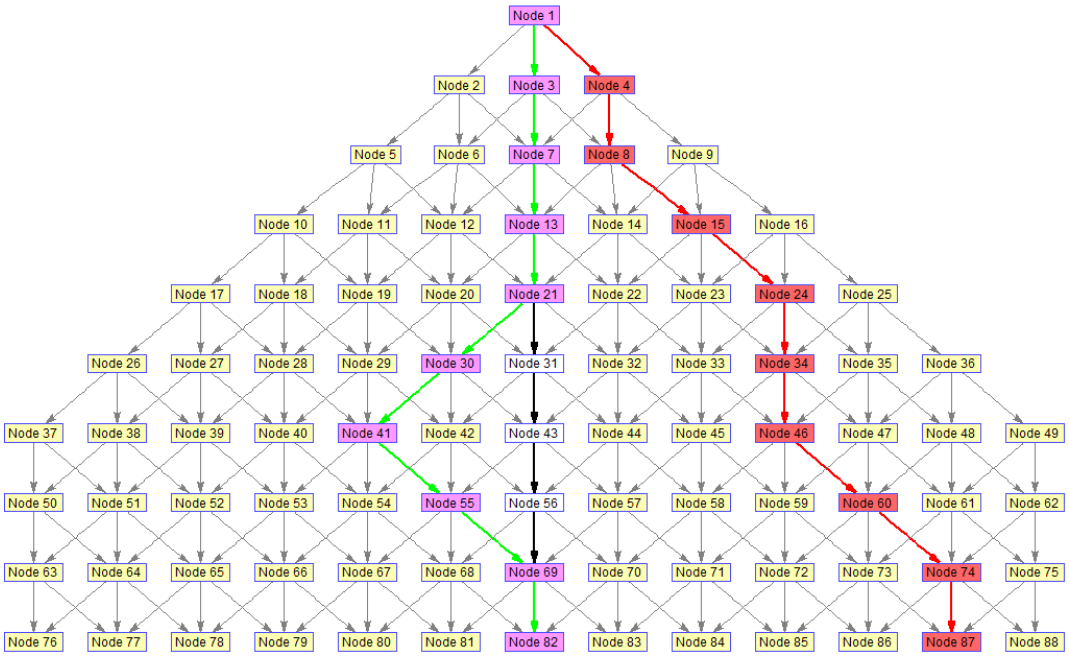

Figure 6.8: The shortest paths calculated using the optimization algorithm generated for the two cases for flight AFR084 on the 28th of February 2013.

The actual flight track flown was 1,049.2 NM in length. The red track, where all exit points were allowed, was however 1,038.5 NM in length or 10.7 NM shorter than the actual track. The red track was therefore 1.0% shorter than the actual track; however it took only 0.4% less time to travel this track compared to the actual track. The green track, where the exit point was fixed as the last waypoint of the actual flight track, was 1,047.8 NM in length or 1.4 NM shorter than the actual track. The green track was 0.1% shorter than the actual track and it took 0.2% less time to travel this track compared to the actual track. The green track was

0.9% longer than the red track but however it only took 0.2% longer to travel the green track. From these results it can be seen that the shorter flight time reached by flying the red path can be attributed to the shorter distance flown. The result for the red path is however limited to this part of the flight only as the distance from the exit point of the red track leads to 75.0 NM or 1.7% longer distance to the arrival airport, compared to the distance from the exit point of the actual flight track. Furthermore, choosing this exit point results in 1.2% longer total distance from entry point to arrival airport compared to the actual track. Choosing the red track would therefore most likely result in higher total flight time than the green track as it only results in 0.2% shorter flight time when compared to flying the green track. However the remaining distance is 1.7% longer.

Figure 6.9 shows the actual flight track compared to the shortest times-paths for the two cases. The black path shown in the figure represents the actual flight path, the red path represents the shortest path, where all exit points were allowed, and the green path represents the shortest path, where the exit point was fixed as the last waypoint of the actual flight track. The green and the red paths are very different and result in different improvement in flight time. The red path finds a better path that is 0.9% shorter than the green track and results in 0.2% shorter traveling time. However, as mentioned, the results of the red path are limited to this part of the flight only as it leads to longer remaining distance.

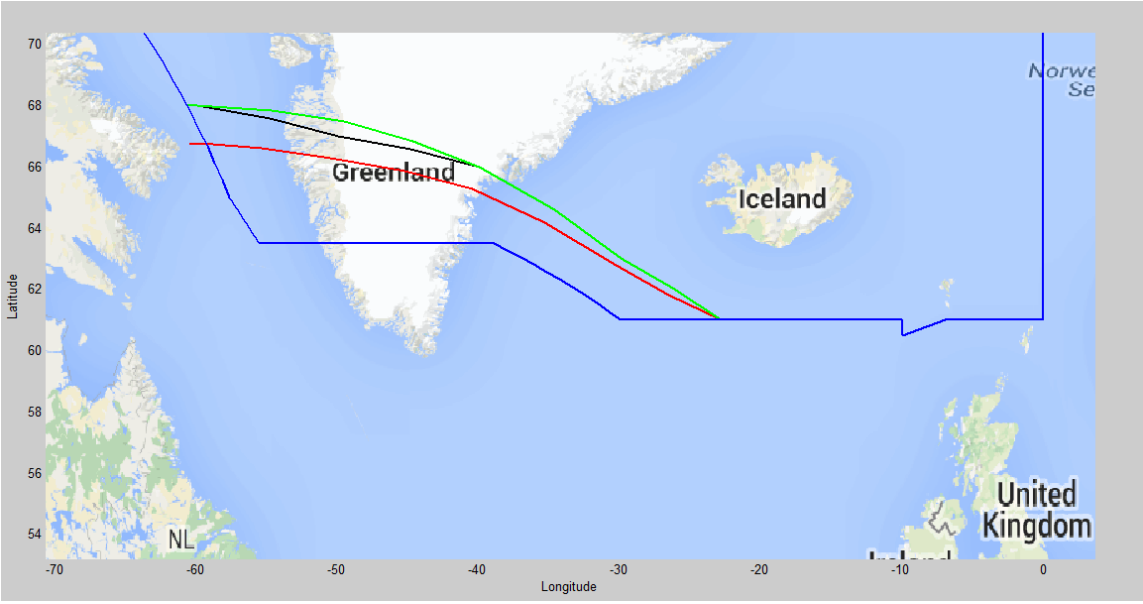

Figure 6.9: The actual flight path and the shortest paths calculated for both cases of flight AFR084. The actual flight path is shown in black, the shortest path if all exit points are allowed is shown in red and the shortest path if the exit point is fixed is shown in green. The area within the blue line represents the Reykjavik CTA.

The BADA fuel consumption model was used to estimate the fuel burn for the aircraft cruise phase. The aircraft was flying at a cruising altitude of 36,000 feet, the aircraft is of the type Boeing 777-200 and the cruising speed in terms of Mach number was 0.84. The nominal weight for Boeing 777-200, which is given in the BADA performance file, was used and equals 208,700 kg. These parameters, along with the mean temperature, were put into the BADA fuel consumption model. Calculated aircraft fuel consumption according to these parameters was 104.2 kg/min. According to these calculations the fuel saved was 35.0 kg when the exit point was fixed and 59.0 kg when all exit points were allowed. These calculations are however not accurate as the exact mass of the aircraft is not known and therefore has to be estimated. The optimization results for flight AFR084 are summarized in Table 6.5.

Table 6.5: Summary of optimization results for flight AFR084.

Case	Improvement in flight time compared to the actual flight path (seconds)	Improvement in flight time compared to the actual flight path (%)	Fuel saved (kg)
Fixed exit point (green path)	20	0.2	35.0
All exit points allowed (red path)	34	0.4	59.0

6.4 Change in Flight Levels

As this study only considers lateral optimization of the flight profile it was decided to determine what the impact would be if the aircraft cruising altitude would be changed. Figure 6.10 shows the fuel consumption rate as a function of altitude for the aircraft types of the three flights optimized, where ISA temperature is assumed. As can be seen in the figure the fuel consumption per minute is very different between the three aircraft types. However, the fuel consumption rate decreases as altitude increases, for all the aircraft types. Because of this feature and also because it was considered interesting to see if there was a significant change in weather conditions between altitudes, it was decided to run the WO algorithm for the two

cases 1,000 feet above and below the cruising altitudes. For the flights PIA781 and AFR084, where the cruising altitude was 36,000 feet, it was therefore decided to run the WO algorithm for a cruising altitude of 35,000 feet and 37,000 feet. For the flight AAL199, where the cruising altitude was 32,000 feet, it was decided to run the WO algorithm for a cruising altitude of 31,000 feet and 33,000 feet. The flight time was calculated using the WO model for three instances; the initial flight track, the shortest time-path where all exit points were allowed and the shortest time-path where the exit point was fixed.

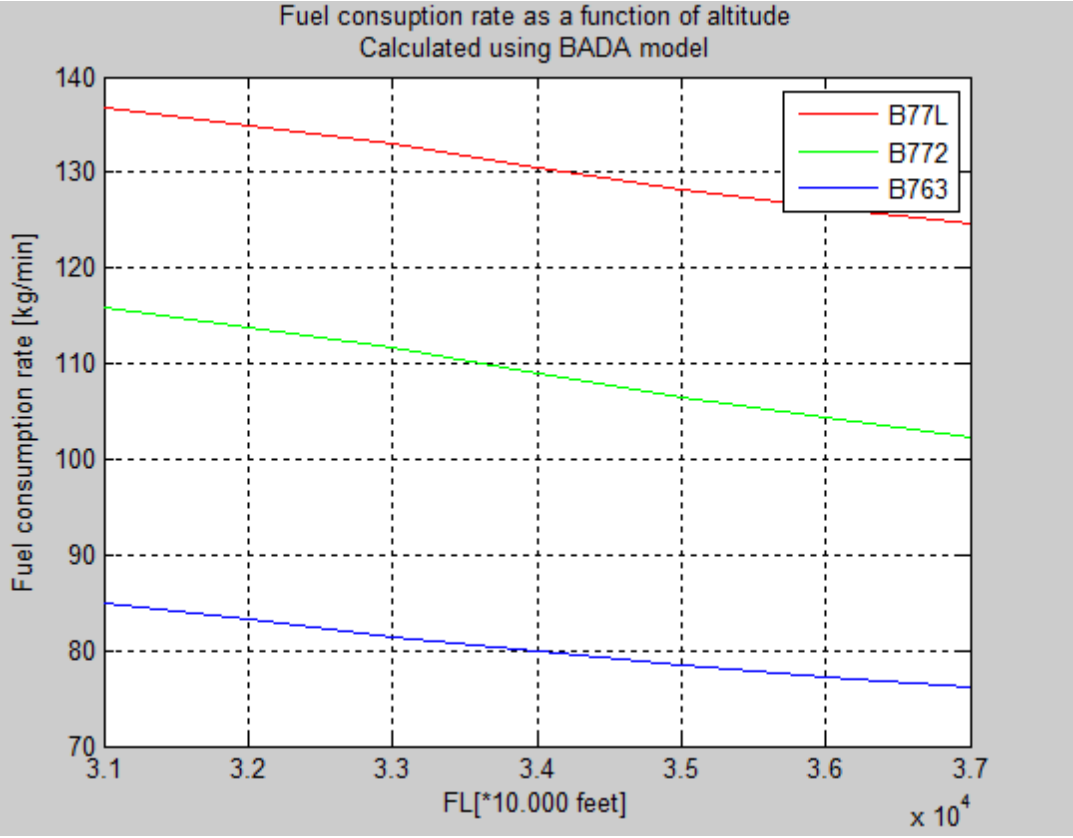

Figure 6.10: Fuel consumption vs. flight level in cruise phase for aircraft types B77L, B772 and B763.

Summarized results for the flight PIA781 at cruising altitudes of 35,000, 36,000 and 37,000 feet can be seen in Table 6.6. As can be seen in the table the flight time was different between cruising altitudes, although the difference was very small, for all cases. The optimization algorithm resulted in the same shortest time-paths for cruising altitudes of 35,000 feet and 36,000 feet, both when the exit point was fixed and when all exit points were allowed. The same paths as showed in Figure 6.2. However the cruising altitude of 37,000 feet resulted in slightly different paths.

Table 6.6: Summarized results for different cruising altitude for flight PIA781.

The initial flight path	35,000 Feet	36,000 feet	37,000 feet
Fuel burn per minute (kg)	127.0	125.2	123.8
Actual flight time according to the WO model if the initial flight path is used (minutes)	284.2	285.2	285.0
Total fuel burn (kg)	36,084.8	35,716.6	35,284.0
All exit points allowed			
Shortest flight time (minutes)	271.8	272.3	271.5
Improvement form initial flight path (minutes)	12.4	12.9	13.5
Improvement form initial flight path (%)	4.4	4.5	4.7
Total fuel burn (kg)	34,515.6	34,104.0	33,616.1
Fuel saved compared to initial flight path (kg)	1,569.2	1,612.6	1,667.9
Exit point fixed			
Shortest flight time (minutes)	279.6	280.5	280.2
Improvement from initial flight path (minutes)	4.6	4.7	4.8
Improvement from initial flight path (%)	1.6	1.6	1.7
Total fuel burn (kg)	35,505.6	35,134.8	34,684.7
Fuel saved compared to initial flight path (kg)	579.2	581.8	599.3

The improvement of flying the shortest time-paths when compared to flying the initial track was highest when flying at a cruising altitude of 37,000 feet. An improvement of 4.7%

compared to an improvement of 4.5% when flying at a cruising altitude of 36,000 feet and 4.4% when flying at a cruising altitude of 35,000 feet. The same applies when the improvement of flying the shortest time-path, when the exit point was fixed as the last waypoint of the actual flight path, is compared to the actual flight track. This resulted in an improvement of 1.7% when flying at a cruising altitude of 37,000 feet compared to an improvement of 1.6% both when flying at cruising altitude of 36,000 feet and 35,000 feet.

The aircraft type of flight PIA781 was Boeing 777-200LR. As can be seen in Figure 6.10 Boeing 777-200LR results in the highest fuel burn per minute, when compared to the other two aircraft types. It can also be seen that the fuel burn decreases as the cruising altitude increases. Therefore, although flying at cruising altitude of 37,000 feet resulted in the highest flight time for two out of three instances, the fuel burn was lowest for all the three instances at this cruising altitude. The reason is that the difference in flight time between altitudes was small when compared to the difference in fuel burn per minute between altitudes. The results showed that flying the initial track at cruising altitude of 37,000 feet resulted in 1.2% less fuel burn when compared to flying the initial track at cruising altitude of 36,000 feet. Flying the shortest time-path where all exit points were allowed at cruising altitude of 37,000 feet resulted in 5.9 % less fuel burn and flying the shortest time-path where the exit point was fixed resulted in 2.9% less fuel, when compared to flying the initial track at cruising altitude of 36,000 feet.

The results were similar when the cruising altitude was changed for the other two flights. For the flight AAL199 the optimization algorithm resulted in the same shortest time-paths when flying at cruising altitudes of 31,000 feet and 32,000 feet, for both cases. The same paths as showed in Figure 6.5. Slightly different shortest time-paths were calculated for cruising altitude of 33,000 feet. The difference in flight time between cruising altitudes was also rather small for flight AAL199. According to the WO model the cruising altitude of 31,000 feet resulted in the shortest flight time when the initial flight track was flown and when the shortest paths were calculated, for both cases. However, flying at a cruising altitude of 33,000 feet resulted in the longest flight time. The flight time increased around 1% per 1,000 feet of altitude.

The improvement in flight time of flying the shortest time-path when all exit points were allowed compared to flying the initial track was highest when flying at a cruising altitude of 33,000 feet. An improvement of 1.1% compared to an improvement of 1.0% when flying at

cruising altitude of 32,000 feet and 31,000 feet. The same applies when the improvement of flying the shortest time-path, when the exit point was fixed as the last waypoint of the initial flight path, was compared to the initial flight track. This resulted in an improvement of 1.1% when flying at a cruising altitude of 33,000 feet compared to an improvement of 1.0% when flying at a cruising altitude of 32,000 feet and 0.9% when flying at a cruising altitude of 31,000 feet.

The aircraft type of flight AAL199 was Boeing 767-300. As can be seen in Figure 6.10 the fuel burn per minute is lowest for Boeing 767-300, when compared to the other two aircraft types, it can also be seen that the fuel burn decreases as the cruising altitude increases. Therefore, flying at a cruising altitude of 33,000 feet resulted in the lowest fuel burn in spite of resulting in the highest flight time. The reason is that the difference in fuel burn rate between altitudes was about twice as high as the difference in flight time between altitudes. The results showed that flying the initial track at a cruising altitude of 33,000 feet resulted in 1.1% less fuel burn when compared to flying the initial track at a cruising altitude of 32,000 feet. Flying the shortest time-paths, for both cases, at a cruising altitude of 33,000 feet resulted however in 2.1 % less fuel burn when compared to flying the initial track at a cruising altitude of 32,000 feet.

For the flight AFR084 the optimization algorithm resulted in the same shortest time-paths as shown in Figure 6.8, for all cruising altitudes, except the case where the exit point was fixed at a cruising altitude of 37,000 feet, which resulted in a slightly different path. The results showed that there was a very small change in flight time between cruising altitudes. According to the WO model the cruising altitude of 35,000 feet resulted in the shortest flight time when the initial flight track was flown and when the shortest paths were calculated, for both cases. The cruising altitude of 37,000 feet however resulted in the longest flight time.

The improvement in flight time of flying the shortest path when all exit points were allowed compared to flying the initial track was highest when flying at a cruising altitude of 35,000 feet. An improvement of 0.5% compared to an improvement of 0.4% both when flying at cruising altitude of 36,000 feet and 37,000 feet. The improvement of flying the shortest time-path, when the exit point was fixed, compared to flying the initial flight track was 0.3% when flying at cruising altitude of 35,000 feet and 37,000 feet and 0.2% when flying at a cruising altitude of 36,000 feet.

The aircraft type of flight AFR084 was Boeing 777-200. As can be seen in Figure 6.10 the fuel burn decreases as the cruising altitude increases, so the fuel burn per minute was lowest when flying at a cruising altitude of 37,000 feet. Therefore, although flying at a cruising altitude of 37,000 feet resulted in the highest flight time, the total fuel burn was the lowest when flying at this cruising altitude. The reason is that the difference in flight time between altitudes was very small when compared to the difference in fuel burn per minute between altitudes. The fuel burn per minute increases about 2.0% when the cruising altitude is decreased to 35,000 feet and decreases about 1.8% when the cruising altitude is increased to 37,000 feet, for this type of aircraft. The results showed that flying the initial track at a cruising altitude of 37,000 feet resulted in 1.8% less fuel burn, when compared to flying the initial track at a cruising altitude of 36,000 feet. Flying the shortest time-paths at a cruising altitude of 37,000 feet resulted however in 2.2 % less fuel burn when all exit points where allowed and 2.0% less fuel burn when the exit point was fixed, when compared to flying the initial track at a cruising altitude of 36,000 feet.

The results are rather similar for all the flights. The results showed that there was small change in weather conditions when the cruising altitude was changed, for all the flights. The main factor that influenced the optimization results was that the fuel burn per minute decreases with increased altitude. The reason is that the difference in flight time between altitudes was very small when compared to the difference in fuel burn per minute between altitudes. That is the reason why flying at the highest cruising altitude always resulted in the lowest fuel burn, although the highest cruising altitude resulted most often in the longest flight time. As temperature decreases with increased altitude this is favorable to aircraft fuel consumption [35].

6.5 More on Flight PIA781

Since the flight PIA781 on 29th of November 2013 resulted in the most fuel savings and because there was a high wind speed that day along with rather high spatial variation of the wind speed, it was decided to optimize more flight tracks on this date. This was done in order to see if the high fuel savings reached in the case of flight PIA781 could lead to the high wind speed and high variation in the wind speed in the area this particular day.

Although there were a large number of flights that flew within BIRD on that day there were not many flights that met the weather data limitations. The flights could only be flying in altitudes of 35,000, 36,000 and 37,000 feet and had to be within the area of the weather data. Additionally, as this study only deals with wind optimization in the lateral plan at a constant cruise altitude, there could be no altitude change in the flight profile. Twelve flights were found on this date that satisfied all these conditions. The difference between the total flight time calculated by running the WO model for the actual flight track and the flight time given in the flight data ranged from 0.5% to 2.6% for these twelve flights. In order to get the most accurate results, the shortest flight time calculated using the WO model was therefore compared to the flight time of the actual track, calculated by using the WO model, as was done for the other three flights. The shortest path was only calculated for the case where the exit point is fixed as the last waypoint of the actual flight track. The results can be seen in Table 6.7. The time needed to fly the shortest time-path, calculated using the WO model, was compared to the time needed to fly the actual flight track. The improvements ranged from 0.3% to 1.8%, where the mean improvement in flight time for these twelve flights was 1.1%. The total fuel saved by flying the wind optimal routes for all the twelve flights was 2,506.1 kg.

Some large airlines like Lufthansa and British Airways, that presumably are using some of the best optimization techniques, result in an improvement of well over 1%, which is considered a significant improvement. Based on these results it can be concluded that the high improvement reached in the flight originally optimized was mainly due to high wind speed and variation in the wind speed. However it has to be kept in mind the weather information the airlines had at the time were probably not as accurate as the weather data used in this study as the weather data obtained from IMR are actual weather that was post processed.

Table 6.7: Summarized results for the 12 flights optimized on 29th of November 2013.

Operator	Flight number	Improvement compared to flying the actual track (%)	Improvement compared to flying the actual track (minutes)	Fuel saved (kg)
Emirates	UAE222	0.4	0.39	49.8
KLM Royal Dutch Airlines	KLM602	1.1	1.61	250.2
El Al - Israel Airlines Ltd	ELY032	1.4	2.15	166.6
Aeroflot - Russian Airlines	AFL103	0.3	0.40	33.4
Air New Zealand	ANZ2	0.5	0.60	80.5
Air Canada	ACA850	1.4	2.32	174.6
British Airways	BAW48	1.8	2.83	427.6
British Airways	BAW84	1.7	2.72	410.5
Finnair	FIN5	0.6	1.80	158.3
Air India Limited	AIC191	0.8	1.94	254.4
KLM Royal Dutch Airlines	KLM602	1.3	1.90	295.7
Deutsche Lufthansa AG	DLH491	1.3	2.46	204.5

Additionally, it was decided to compare the distance of the twelve flight tracks optimized to the improvement in flight time. This was done to see if the distance of the flight tracks optimized influenced the improvement in flight time in that way that longer flight tracks would result in more improvement in flight time. As can be seen in Figure 6.11 the shortest flight tracks resulted in the lowest improvements and as the distance of the flight tracks increased the improvement also increased. However, as can be seen in the figure the two flight tracks which were significantly longer than the other flight tracks resulted in low improvement. The results indicate that there is some connection between the length of the optimized flight tracks and the improvement achieved, however there is clearly some inconsistency.

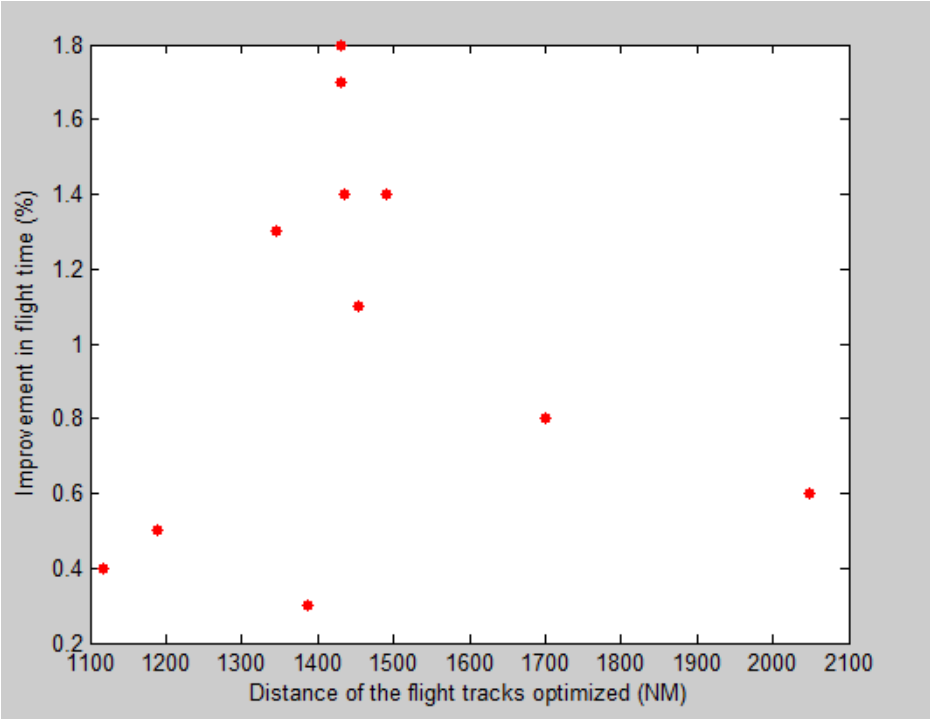

Figure 6.11: The improvement in flight time compared to the distance of the flight tracks optimized.

6.6 Emissions

Minimizing aircraft fuel consumptions by flying wind optimal routes subsequently leads to minimization of emissions. The standard emission convertor factor used to convert jet fuel into CO_2 is 3.155 [36], which means that 1 kg of consumed jet fuel produces 3.155 kg of CO_2. As the aviation industry is a large consumer of fossil fuels only a small rate of fuel burn reduction, like the one achieved in this study, would add up to a substantial amount of CO_2 emission savings. Operational improvements, like increasing fuel efficiency by optimizing aircraft tracks, are therefore a step into making aviation a more environmentally friendly industry. If only the case where the exit point is fixed is considered, the fuel savings of the three flights initially optimized could potentially have saved 2,263 kg of CO_2. The twelve flights optimized on 29th of November resulted in total fuel savings of 2,506 kg which leads to potential of 7,907 kg of CO_2 savings.

Chapter 7

Summary and Conclusions

Increasing fuel efficiency has become an increasingly important factor in the aviation industry. The main reason is that fuel is a major factor in airlines operating expenditures. Fuel price has been rising in recent years and is expected to continue rising in coming years. In addition to this, there has been increased awareness of the impact of man-made climate changes. The introduction of the European Union of carbon charges has also led to an additional cost item for airlines.

In this study an optimization algorithm was developed which calculates the shortest path in terms of time of flight for aircraft in the cruise phase by optimizing flight trajectories with respect to nowcasting of the winds aloft. The optimization algorithm used was the Dijkstra shortest path algorithm. A geographical grid was constructed around the actual flight track, where the new waypoints were perpendicular to the actual flight track. The grid was used to deviate from the actual flight track. The aircraft deviates in the lateral plane from the actual flight track if it results in shorter flight time, when compared to the time it takes to fly the actual flight track. When deviating from the actual flight track, the distance might be significantly longer than the distance of the actual flight track. Therefore the weather condition have to be favorable in that way that the wind speed and wind direction lead to time saved, although the distance flown might be longer. The shortest time-path was found for two cases defining the first waypoint of the actual flight track as the starting point. In the first case all the exit points of the grid were allowed but in the second case the last waypoint of the actual flight track was allowed as an exit point. The flight tracks considered in this study were mainly within BIRD.

Three flights were initially considered, flight PIA781 on 29th of November 2013, flight AAL199 on 9th of October 2013 and flight AFR084 on 28th of February 2013. The upper bound on fuel burn and emission reduction for these flights was 4.5% when all exit points where allowed and 1.6% when the exit point was fixed. The three flights however resulted in very different results, ranging from 0.2% to 4.5% reduction in fuel burn and emission. The high improvement for the case when all exit points were allowed is however not descriptive for the improvement reachable in reality. The reason is that airlines cannot always choose the

exit point as the exit point is often fixed by ATC because of requirements of entry point into next ATC area. Furthermore, a high improvement reached when all exit points are allowed can be misleading as the largest part of the improvement can often be attributed to reduced distance flown within BIRD. The reduced distance is however limited to the part of the flight profile which is being optimized and often leads to the remaining distance to be significantly longer, when compared to the remaining distance from the last waypoint of the actual track. When the flight profile from entry point to arrival airport is taken into consideration, the improvement when all exit points are allowed can therefore be less than the improvement when the exit point is fixed.

The lateral trajectories were also optimized 1,000 feet above and below the actual flight level, for each of the three flights initially optimized. The results showed that there was not a major change in weather conditions when the altitude was changed, for any of the flights. The altitude changes only resulted in a small difference in flight time for all the three flights. The main factor that influenced the optimization results was however that the fuel burn per minute decreases with increased altitude. The reason is that the difference in flight time between altitudes was very small when compared to the difference in fuel burn per minute between altitudes. Therefore, although the highest cruising altitude resulted most often in the longest traveling time for these three flights, the total fuel burn was always the lowest when the highest altitude was chosen. As temperature decreases with increased altitude this is favorable to aircraft fuel consumption [35].

Flight PIA781 on 29th of November 2013 resulted in more significant reduction of fuel burn than the other two flights. It was therefore considered interesting to see if this was just a coincidence or whether the weather conditions on this day made it hard for airlines in general to optimize the flight tracks with respect to wind. For this reason the track for twelve more flights were optimized on that day by determining, the shortest time-path for the case where the exit point was fixed. The improvements in flight time, when compared to the time it took to travel the actual flight track, ranged from 0.3% to 1.8%, where the mean improvement in flight time was 1.1%. When these results are compared to the improvement for flight PIA781, which was 1.6%, it can be concluded that the main reason for the improvement was the weather conditions.

This research is a follow up of an MS project titled Lateral Optimization of Aircraft Tracks in Reykjavik Air Traffic Control Area [7]. The improvement achieved in this study was of

similar magnitude as the improvement reached in the former study, which resulted in close to 1% fuel burn when compared to the fuel consumption estimated for the cruise phase by the flight plan. Both of these research focused on the flight within the Reykjavik Control Area, although the two flight that were examined in the former study only flew in part of the area whereas in this current study all flights examined flew all the way through the area. Moreover, the former study only considered flights in the summer while this current study only considered flights in the winter. Both studies indicate that there is promising potential for improvements in lateral trajectory optimization. In this current study total fifteen flights were optimized, which all showed some potential for reduction in fuel burn and thereby emission to be reduced via simple lateral trajectory change, where more wind optimal routes are chosen.

7.1 Future Research

Future research could attain increased fuel efficiency by considering both lateral and vertical optimization of the flight profile. That is, by taking advantage of tailwind or decreasing the impact of the headwind with both altitude and lateral trajectory changes. It would be interesting to see the improvement this would result in compared to the improvement achieved in this current study, where only lateral optimization of the flight profile was considered. It would be preferable to perform the optimization for the whole flight profile, instead of just a part of the cruising phase. To get as reliable results as possible of the achievable fuel savings over a whole year more flights would have to be considered, where flights that are more descriptive for the whole year would be chosen. For instance, at least one flight in each month of the year would be optimized. Moreover future research should consider more diverse flights, which can be achieved by receiving data from more than one airline. These modifications should lead to results that are more accurate of the potential benefit reachable over a period of one year if all trajectories would be optimized.

References

[1] International Air Transport Association (IATA), "FACT SHEET: Fuel," Dec-2013. [Online]. Available: http://www.iata.org/pressroom/facts_figures/fact_sheets/Documents/fuel-fact-sheet.pdf. [Accessed: 16-Apr-2014].

[2] R. L. Hirsch, R. H. Bezdek, and R. M. Wendling, "Peaking of world oil production: impacts, mitigation and risk management," Feb. 2005.

[3] A. Maurya, "Environmental Impact of the Flying Scenario: An Approach Towards Sustainable Air Transportation: A Case Study of India," Social Science Research Network, Rochester, NY, SSRN Scholarly Paper ID 2333269, Sep. 2013.

[4] International Air Transport Association (IATA), "Passenger Demand Maintains Historic Growth Rates in 2013." [Online]. Available: http://www.iata.org/pressroom/pr/Pages/2014-02-06-01.aspx. [Accessed: 14-May-2013].

[5] R. Kar, P. A. Bonnefoy, and R. J. Hansman, "Dynamics of implementation of mitigating measures to reduce CO_2 emissions from commercial aviation," Massachusetts Institute of Technology, 2010.

[6] W. Roberson, R. Root, and D. Adams, "Fuel Conservation Strategies: Cruise Flight," *Boeing Fourth–quarter*, 2007.

[7] E. I. Andrésson, "Lateral Optimization of Aircraft Tracks in Reykjavik Air Traffic Control Area," Reykjavik University, 2012.

[8] Isavia, "Flugtölur 2013," Isavia, Reykjavíkurflugvöllur, 101 Reykjavík Iceland, 2014.

[9] International Air Transport Association (IATA), "Fuel Price Analysis." [Online]. Available: http://www.iata.org/publications/economics/fuel-monitor/Pages/price-analysis.aspx.

[10] J. P. Rafferty, *Climate and Climate Change*. Bitannica Educational Publishing, 2011.

[11] E. O'Toole, "The Jetstream and The Weather in the UK." [Online]. Available: http://www.netweather.tv/index.cgi?action=jetstream-tutorial;sess=. [Accessed: 04-May-2014].

[12] NOAA Earth System Research Laboratory, Physical Sciences Division, "ESRL : PSD : Daily Climate Composites." [Online]. Available: http://www.esrl.noaa.gov/psd/data/composites/day/. [Accessed: 12-Apr-2014].

[13] H. Pálsson, "Reduction of Emissions on the North Atlantic by the Implementation of ADS-B," Reykjavíkurflugvöllur, 101 Reykjavík Iceland, Apr. 2010.

[14]“Performance of Flight Trials and Demonstrations Validating Solutions for the Reduction of CO2 Emissions,” Sesar Joint Undertaking, Nov. 2011.

[15]H. K. Ng, B. Sridhar, S. Grabbe, and N. Chen, “Cross-polar aircraft trajectory optimization and the potential climate impact,” in *Digital Avionics Systems Conference (DASC), 2011 IEEE/AIAA 30th*, 2011.

[16]Isavia, “REYKJAVIK CONTROL AREA.” [Online]. Available: http://www.isavia.is/english/air-navigation/reykjavik-area-control-centre/reykjavik-control-area/. [Accessed: 16-Apr-2014].

[17]Þ. Pálsson, “Personal Communications,” Apr-2014.

[18]Isavia, “ADS-B.” [Online]. Available: http://www.isavia.is/english/air-navigation/ads-b/. [Accessed: 16-Apr-2014].

[19]“Datalink – a long time coming,” *NATS Blog*. [Online]. Available: http://nats.aero/blog/2014/01/datalink-long-time-coming/. [Accessed: 12-Apr-2014].

[20]H. Pálsson, “Data links,” Personal e-mail (May 30, 2014).

[21]S. de Haan, L. J. Bailey, and J. E. Können, “Quality assessment of Automatic Dependent Surveillance Contract (ADS-C) wind and temperature observation from commercial aircraft,” Feb. 2013.

[22]C. Nutt, “NATS Fuel Efficiency Metric,” NATS, Jan. 2012.

[23]EUROCONTROL, “Base of Aircraft Data (BADA).” [Online]. Available: https://www.eurocontrol.int/services/bada. [Accessed: 13-Apr-2014].

[24]T. H. Cormen, R. L. Rivest, S. Clifford, and C. E. Leiserson, *Introduction to algorithms*, 3rd edition. Cambridge, Mass.: MIT Press, 2009.

[25]S. S. Skiena, *The Algorithm Design Manual*, 2nd edition. Springer, 2008.

[26]E. W. Weisstein, “Adjacency Matrix -- from Wolfram MathWorld.” [Online]. Available: http://mathworld.wolfram.com/AdjacencyMatrix.html. [Accessed: 13-Apr-2014].

[27]E. W. Weisstein, “Great Circle -- from Wolfram MathWorld.” [Online]. Available: http://mathworld.wolfram.com/GreatCircle.html. [Accessed: 12-Apr-2014].

[28]E. W. Weisstein, “Spherical Coordinates -- from Wolfram MathWorld.” [Online]. Available: http://mathworld.wolfram.com/SphericalCoordinates.html. [Accessed: 14-May-2014].

[29]“Navigation Principles.” [Online]. Available: http://www.free-online-private-pilot-ground-school.com/navigation-principles.html. [Accessed: 12-Apr-2014].

[30]“True, Equivalent, and Calibrated Airspeeds.” [Online]. Available: http://www.mathpages.com/home/kmath282/kmath282.htm. [Accessed: 16-Apr-2014].

[31]E. P. Kolano, “PILOT’S OPERATING HANDBOOK AND FAA APPROVED AIRPLANE FLIGHT MANUAL,” Mar. 2006.

[32]G. Darby, “Wind Triangle,” 15-Jan-2011. [Online]. Available: http://delphiforfun.org/Programs/Math_Topics/WindTriangle.htm.

[33]The MathWorks, Inc., “Mapping Toolbox™ User’s Guide.” Sep-2013.

[34]B. K. Stefánsson and H. Pálsson, “Analyses of the Speed Distribution of Aircraft that have an Assigned Mach Speed.” Oct-2013.

[35]Specific Range Solutions Ltd., “Parametric Specific Fuel Consumption Analysis of the PW120A Turboprop Engine,” Jul. 2009.

[36]D. J. Parsons, J. C. Chatterton, and J. R. Nicholls, “Carbon Brainprint Case Study: ceramic coatings for jet engine turbine blades,” Report, Jul. 2011.

Appendices

Appendix A Matlab Code for the Construction of the Grid

```
%% Calculate coordinates for the grid

function [grid, Longitude, Latitude] =
grid_FP_general_detailedWeather(Longitude_flightplan, Latitude_flightplan)

Longitude_flightplan =  [-22.8742 -30.0000  -40.0000  -50.0000  -60.0000  -60.7639]';
Latitude_flightplan = [61.0000   63.0000   66.0000   67.0000   68.0000   67.9839]';

[az,dist] = legs(Latitude_flightplan,Longitude_flightplan, 'gc')

% Add new waypoints if GCD > 100 nm
New_GCD = dist/2;

[latout,lonout] = reckon(Latitude_flightplan(1:(length(Longitude_flightplan(:))-1)),
Longitude_flightplan(1:(length(Longitude_flightplan(:))-1)),nm2deg(New_GCD),az)

new_lat_matrix=[];
new_lon_matrix=[];
n = length(Latitude_flightplan(:,1));
for i = 1: n-1
   if dist(i) > 100
      new_lat = [Latitude_flightplan(i),latout(i)]
      new_lon = [Longitude_flightplan(i),lonout(i)]
      else
      new_lat = [Latitude_flightplan(i)]
      new_lon = [Longitude_flightplan(i)]
   end
   new_lat_matrix=[new_lat_matrix new_lat]
   new_lon_matrix = [new_lon_matrix new_lon]
end
```

```
Longitude =  [new_lon_matrix,Longitude_flightplan(end,1)]
Latitude =  [new_lat_matrix, Latitude_flightplan(end,1)]

% Calculate the new coordinates
k = length(Longitude(1,:))-1;

for j = 1:k
    % Adjust the coordinates with cosine of typical latitude
    adjusted_flightplan1 = [Longitude(j)'* cosd(((Latitude(j+1)+Latitude(j))/2)),
    Latitude(j)'];
    adjusted_flightplan2 = [Longitude(j+1)'* cosd(((Latitude(j+1)+Latitude(j))/2)),
    Latitude(j+1)'];

    % The direction vector
    v = [adjusted_flightplan2 - adjusted_flightplan1];

    % The direction vector is turned at right angles clockwise to produce a
    % perpendicular direction to the right
    w = [v(2), -v(1)];

    %Calculating the length of the vector
    length_of_w = sqrt(w(1)^2 + w(2)^2);

    % The new coordinates generated
    displacement_1 = adjusted_flightplan1 + 1.5/length_of_w* w;
    displacement_2 = adjusted_flightplan1 + 1.25/length_of_w* w;
    displacement_3 = adjusted_flightplan1 + 1/length_of_w* w;
    displacement_4 = adjusted_flightplan1 + 0.75/length_of_w* w;
    displacement_5 = adjusted_flightplan1 + 0.5/length_of_w* w;
    displacement_6 = adjusted_flightplan1 + 0.25/length_of_w* w;
    displacement_7 = adjusted_flightplan1 + -0.25/length_of_w* w;
    displacement_8 = adjusted_flightplan1 + -0.5/length_of_w* w;
    displacement_9 = adjusted_flightplan1 + -0.75/length_of_w* w;
    displacement_10 = adjusted_flightplan1 + -1/length_of_w* w;
```

```
displacement_11 = adjusted_flightplan1 + -1.25/length_of_w* w;
displacement_12 = adjusted_flightplan1 + -1.5/length_of_w* w;

displacement_lastPoint1 = adjusted_flightplan2 + 1.5/length_of_w* w;
displacement_lastPoint2 = adjusted_flightplan2 + 1.25/length_of_w* w;
displacement_lastPoint3 = adjusted_flightplan2 + 1/length_of_w* w;
displacement_lastPoint4 = adjusted_flightplan2 + 0.75/length_of_w* w;
displacement_lastPoint5 = adjusted_flightplan2 + 0.5/length_of_w* w;
displacement_lastPoint6 = adjusted_flightplan2 + 0.25/length_of_w* w;
displacement_lastPoint7 = adjusted_flightplan2 + -0.25/length_of_w* w;
displacement_lastPoint8 = adjusted_flightplan2 + -0.5/length_of_w* w;
displacement_lastPoint9 = adjusted_flightplan2 + -0.75/length_of_w* w;
displacement_lastPoint10 = adjusted_flightplan2 + -1/length_of_w* w;
displacement_lastPoint11 = adjusted_flightplan2 + -1.25/length_of_w* w;
displacement_lastPoint12 = adjusted_flightplan2 + -1.5/length_of_w* w;

% Adjusting the coordinates again
undo_adjustment_1 = [displacement_1(1)/cosd(((Latitude(j+1)+Latitude(j))/2)),
displacement_1(2)];
undo_adjustment_2 = [displacement_2(1)/cosd(((Latitude(j+1)+Latitude(j))/2)),
displacement_2(2)];
undo_adjustment_3 = [displacement_3(1)/cosd(((Latitude(j+1)+Latitude(j))/2)),
displacement_3(2)];
undo_adjustment_4 = [displacement_4(1)/cosd(((Latitude(j+1)+Latitude(j))/2)),
displacement_4(2)];
undo_adjustment_5 = [displacement_5(1)/cosd(((Latitude(j+1)+Latitude(j))/2)),
displacement_5(2)];
undo_adjustment_6 = [displacement_6(1)/cosd(((Latitude(j+1)+Latitude(j))/2)),
displacement_6(2)];
undo_adjustment_7 = [displacement_7(1)/cosd(((Latitude(j+1)+Latitude(j))/2)),
displacement_7(2)];
undo_adjustment_8 = [displacement_8(1)/cosd(((Latitude(j+1)+Latitude(j))/2)),
displacement_8(2)];
undo_adjustment_9 = [displacement_9(1)/cosd(((Latitude(j+1)+Latitude(j))/2)),
```

```
displacement_9(2)];
undo_adjustment_10 = [displacement_10(1)/cosd(((Latitude(j+1)+Latitude(j))/2)),
displacement_10(2)];
undo_adjustment_11 = [displacement_11(1)/cosd(((Latitude(j+1)+Latitude(j))/2)),
displacement_11(2)];
undo_adjustment_12 = [displacement_12(1)/cosd(((Latitude(j+1)+Latitude(j))/2)),
displacement_12(2)];

undo_adjustment_lastPoint1 = [displacement_lastPoint1(1)/cosd(((Latitude(j+1) +
Latitude(j))/2)), displacement_lastPoint1(2)];
undo_adjustment_lastPoint2 = [displacement_lastPoint2(1)/cosd(((Latitude(j+1)+
Latitude(j))/2)), displacement_lastPoint2(2)];
undo_adjustment_lastPoint3 = [displacement_lastPoint3(1)/cosd(((Latitude(j+1)+
Latitude(j))/2)), displacement_lastPoint3(2)];
undo_adjustment_lastPoint4 = [displacement_lastPoint4(1)/cosd(((Latitude(j+1)+
Latitude(j))/2)), displacement_lastPoint4(2)];
undo_adjustment_lastPoint5 = [displacement_lastPoint5(1)/cosd(((Latitude(j+1)+
Latitude(j))/2)), displacement_lastPoint5(2)];
undo_adjustment_lastPoint6 = [displacement_lastPoint6(1)/cosd(((Latitude(j+1)+
Latitude(j))/2)), displacement_lastPoint6(2)];
undo_adjustment_lastPoint7 = [displacement_lastPoint7(1)/cosd(((Latitude(j+1)+
Latitude(j))/2)), displacement_lastPoint7(2)];
undo_adjustment_lastPoint8 = [displacement_lastPoint8(1)/cosd(((Latitude(j+1)+
Latitude(j))/2)), displacement_lastPoint8(2)];
undo_adjustment_lastPoint9 = [displacement_lastPoint9(1)/cosd(((Latitude(j+1)+
Latitude(j))/2)), displacement_lastPoint9(2)];
undo_adjustment_lastPoint10 =[displacement_lastPoint10(1)/cosd(((Latitude(j+1)+
Latitude(j))/2)), displacement_lastPoint10(2)];
undo_adjustment_lastPoint11 =[displacement_lastPoint11(1)/cosd(((Latitude(j+1)+
Latitude(j))/2)), displacement_lastPoint11(2)];
undo_adjustment_lastPoint12 =[displacement_lastPoint12(1)/cosd(((Latitude(j+1)+
Latitude(j))/2)), displacement_lastPoint12(2)];

perpendicular_1(:,j) = undo_adjustment_1;
```

```
    perpendicular_2(:,j) = undo_adjustment_2;
    perpendicular_3(:,j) = undo_adjustment_3;
    perpendicular_4(:,j) = undo_adjustment_4;
    perpendicular_5(:,j) = undo_adjustment_5;
    perpendicular_6(:,j) = undo_adjustment_6
    perpendicular_7(:,j) = undo_adjustment_7;
    perpendicular_8(:,j) = undo_adjustment_8;
    perpendicular_9(:,j) = undo_adjustment_9;
    perpendicular_10(:,j) = undo_adjustment_10;
    perpendicular_11(:,j) = undo_adjustment_11;
    perpendicular_12(:,j) = undo_adjustment_12;

    perpendicular_lastPoint1(:,j) = undo_adjustment_lastPoint1;
    perpendicular_lastPoint2(:,j) = undo_adjustment_lastPoint2;
    perpendicular_lastPoint3(:,j) = undo_adjustment_lastPoint3;
    perpendicular_lastPoint4(:,j) = undo_adjustment_lastPoint4;
    perpendicular_lastPoint5(:,j) = undo_adjustment_lastPoint5;
    perpendicular_lastPoint6(:,j) = undo_adjustment_lastPoint6;
    perpendicular_lastPoint7(:,j) = undo_adjustment_lastPoint7;
    perpendicular_lastPoint8(:,j) = undo_adjustment_lastPoint8;
    perpendicular_lastPoint9(:,j) = undo_adjustment_lastPoint9;
    perpendicular_lastPoint10(:,j) = undo_adjustment_lastPoint10;
    perpendicular_lastPoint11(:,j) = undo_adjustment_lastPoint11;
    perpendicular_lastPoint12(:,j) = undo_adjustment_lastPoint12;
end

% The new lat and lon
lon_1 = [perpendicular_1(1,:), undo_adjustment_lastPoint1(1)];
lat_1 = [perpendicular_1(2,:), undo_adjustment_lastPoint1(2)];
lon_2 = [perpendicular_2(1,:), undo_adjustment_lastPoint2(1)];
lat_2 = [perpendicular_2(2,:), undo_adjustment_lastPoint2(2)];
lon_3 = [perpendicular_3(1,:), undo_adjustment_lastPoint3(1)];
lat_3 = [perpendicular_3(2,:), undo_adjustment_lastPoint3(2)];
lon_4 = [perpendicular_4(1,:), undo_adjustment_lastPoint4(1)];
```

```
lat_4 = [perpendicular_4(2,:), undo_adjustment_lastPoint4(2)];
lon_5 = [perpendicular_5(1,:), undo_adjustment_lastPoint5(1)];
lat_5 = [perpendicular_5(2,:), undo_adjustment_lastPoint5(2)];
lon_6 = [perpendicular_6(1,:), undo_adjustment_lastPoint6(1)];
lat_6 = [perpendicular_6(2,:), undo_adjustment_lastPoint6(2)];
lon_7 = [perpendicular_7(1,:), undo_adjustment_lastPoint7(1)];
lat_7 = [perpendicular_7(2,:), undo_adjustment_lastPoint7(2)];
lon_8 = [perpendicular_8(1,:), undo_adjustment_lastPoint8(1)];
lat_8 = [perpendicular_8(2,:), undo_adjustment_lastPoint8(2)];
lon_9 = [perpendicular_9(1,:), undo_adjustment_lastPoint9(1)];
lat_9 = [perpendicular_9(2,:), undo_adjustment_lastPoint9(2)];
lon_10 = [perpendicular_10(1,:), undo_adjustment_lastPoint10(1)];
lat_10 = [perpendicular_10(2,:), undo_adjustment_lastPoint10(2)];
lon_11 = [perpendicular_11(1,:), undo_adjustment_lastPoint11(1)];
lat_11 = [perpendicular_11(2,:), undo_adjustment_lastPoint11(2)];
lon_12 = [perpendicular_12(1,:), undo_adjustment_lastPoint12(1)];
lat_12 = [perpendicular_12(2,:), undo_adjustment_lastPoint12(2)];

% The grid constructed
grid = [ lat_1', lon_1', lat_2', lon_2', lat_3', lon_3', lat_4', lon_4', lat_5', lon_5', lat_6',
lon_6', Latitude', Longitude', lat_7', lon_7', lat_8', lon_8', lat_9', lon_9', lat_10',
lon_10', lat_11', lon_11', lat_12', lon_12' ]

% The empty nodes defined as nan
grid(1:1,1:12) = nan
grid(1:1,15:26) = nan
grid(2:2,1:10) = nan
grid(2:2,17:26) = nan
grid(3:3,1:8) = nan
grid(3:3,19:26) = nan
grid(4:4,1:6) = nan
grid(4:4,21:26) = nan
grid(5:5,1:4) = nan
grid(5:5,23:26) = nan
```

```
grid(6:6,1:2) = nan
grid(6:6,25:26) = nan

% Plotting the grid
figure(1)
axis([-70 0 30 100])
hold on
plot(grid(:,2),grid(:,1),'.g')
hold on
plot(grid(:,4),grid(:,3),'.b')
hold on
plot(grid(:,6),grid(:,5),'.y')
hold on
plot(grid(:,8),grid(:,7),'.r')
hold on
plot(grid(:,10),grid(:,9),'.c')
hold on
plot(grid(:,12),grid(:,11),'.m')
hold on
plot(grid(:,14),grid(:,13),'.k')
hold on
plot(grid(:,16),grid(:,15),'.m')
hold on
plot(grid(:,18),grid(:,17),'.c')
hold on
plot(grid(:,20),grid(:,19),'.r')
hold on
plot(grid(:,22),grid(:,21),'.y')
hold on
plot(grid(:,24),grid(:,23),'.b')
hold on
plot(grid(:,26),grid(:,25),'.g')
end
```

Appendix B Matlab Code for the Adjacency Matrix

```
%% The adjacency matrix
[grid, Longitude, Latitude] = grid_FP_general_detailedWeather(Longitude_flightplan,
Latitude_flightplan)

N = length(grid(:,1))*(length(grid(1,:))/2)-12-10-8-6-4-2;
M = length(grid(:,1))*(length(grid(1,:))/2)-12-10-8-6-4-2;
adj_detailedWeather = zeros(N,M);

for N = 1:M
   if N==1
      adj_detailedWeather(1,2:4)= 1;
   elseif N>=2 && N<=4
            adj_detailedWeather(N,(N+3))=1;
            adj_detailedWeather(N,(N+4))=1;
            adj_detailedWeather(N,(N+5))=1;
    elseif N>=5 && N<=9
            adj_detailedWeather(N,(N+5))=1;
            adj_detailedWeather(N,(N+6))=1;
            adj_detailedWeather(N,(N+7))=1;
    elseif N>=10 && N<=16
            adj_detailedWeather(N,(N+7))=1;
            adj_detailedWeather(N,(N+8))=1;
            adj_detailedWeather(N,(N+9))=1;
    elseif N>=17 && N<=25
            adj_detailedWeather(N,(N+9))=1;
            adj_detailedWeather(N,(N+10))=1;
            adj_detailedWeather(N,(N+11))=1;
    elseif N>=26 && N<=36
            adj_detailedWeather(N,(N+11))=1;
            adj_detailedWeather(N,(N+12))=1;
            adj_detailedWeather(N,(N+13))=1;
    elseif ~isempty(find(N == 37:13:M-25)) == true
```

```
            adj_detailedWeather(N,N+13)=1;
            adj_detailedWeather(N,N+14)=1;
        elseif ~isempty(find(N == 49:13:M-13 )) == true
            adj_detailedWeather(N,N+12)=1;
            adj_detailedWeather(N,N+13)=1;
        elseif N<=M-14
            adj_detailedWeather(N,N+12)=1;
            adj_detailedWeather(N,N+13)=1;
            adj_detailedWeather(N,N+14)=1;
    end
end
```

Appendix C Matlab Code for the Algorithm

```
%% Flight FP_2013_Nov{1,9748}
% Date: 29 Nov 2013
% Operator: Pakistan International Airlines Corporation
% Aircraft type: B77L
% DepAero: OPRN
% ArrAero: CYYZ
% Mach speed: 0.83
% Altitude: 36000

Flight = FP_2013_Nov{1,9748};
Altitude = Flight.Waypoints.Altitude(1);
K = 273.15;
T = K + mean_Temp;
Mach_speed = Flight.Waypoints.mach_speed(1);

%% Coordinates for grid
[grid, Longitude, Latitude] = grid_FP_general_detailedWeather(Longitude_flightplan,
Latitude_flightplan);
%% Create Great circle distance matrix and course matrix
course_matrix1 = [];
dist_matrix1 = [];
for s = 1:2:length(grid(1,:))-1
      [coursegcd, distgcd] = legs(grid(:,s), grid(:,s+1), 'gc') ;
  course_matrix1 = [course_matrix1 coursegcd];
  dist_matrix1 = [dist_matrix1 distgcd];
end

course_matrix = [course_matrix1];
dist_matrix = [dist_matrix1];

% Columns 1, 4, 7, 10, 13, 16, 19, 22, 25, 28, 31, 34 and 37 in GCD matrix
straight_edges = dist_matrix;
```

```
% Columns 1, 4, 7, 10, 13, 16, 19, 22, 25, 28, 31, 34 and 37 in course matrix
course_straight_edges = course_matrix;

% Find angled edges from left to right
lat_angled_edges_matrix1 = [];
lon_angled_edges_matrix1 = [];
for s = 1:2:length(grid(1,:))-3
   for n = length(grid(:,1));
      lat1_angled_edges = [grid(1:n-1,s), grid(2:n,s+2)];
      lat_angled_edges = reshape(lat1_angled_edges.',1,(n-1)*2);

      lon1_angled_edges = [grid(1:n-1,s+1), grid(2:n,s+3)];
      lon_angled_edges = reshape(lon1_angled_edges.',1,(n-1)*2);
   end

      lat_angled_edges_matrix1 = [lat_angled_edges_matrix1; lat_angled_edges ];
      lon_angled_edges_matrix1 = [lon_angled_edges_matrix1; lon_angled_edges ];
end

lat_angled_edges_matrix = [lat_angled_edges_matrix1];
lon_angled_edges_matrix = [lon_angled_edges_matrix1];

course_gcd_angled1 =[];
dist_gcd_angled1 =[];
for j = 1:length(lat_angled_edges_matrix(:,1));
   [coursegcd_angled1, distgcd_angled1] = legs(lat_angled_edges_matrix(j,:),
   lon_angled_edges_matrix(j,:), 'gc');

   course_gcd_angled1 =[course_gcd_angled1 coursegcd_angled1];
   dist_gcd_angled1 =[dist_gcd_angled1 distgcd_angled1];
end

course_gcd_angled =[course_gcd_angled1];
```

```
dist_gcd_angled =[dist_gcd_angled1];

% Find angled edges from right to left
lat_angled_edges_matrix2 = [];
lon_angled_edges_matrix2 = [];
for s = 1:2:length(grid(1,:))-3
   for n = length(grid(:,1))
      lat1_angled_edges2 = [grid(1:n-1,s+2), grid(2:n,s)];
      lat_angled_edges2 = reshape(lat1_angled_edges2.',1,(n-1)*2);

      lon1_angled_edges2 = [grid(1:n-1,s+3), grid(2:n,s+1)];
      lon_angled_edges2 = reshape(lon1_angled_edges2.',1,(n-1)*2);
   end

      lat_angled_edges_matrix2 = [lat_angled_edges_matrix2; lat_angled_edges2 ];
      lon_angled_edges_matrix2 = [lon_angled_edges_matrix2; lon_angled_edges2 ];
end

lat_angled_edges_matrix2 = [lat_angled_edges_matrix2];
lon_angled_edges_matrix2 = [lon_angled_edges_matrix2];

course_gcd_angled12 =[];
dist_gcd_angled12 =[];
for j = 1:length(lat_angled_edges_matrix2(:,1))
   [coursegcd_angled2, distgcd_angled2] = legs(lat_angled_edges_matrix2(j,:),
   lon_angled_edges_matrix2(j,:), 'gc');

   course_gcd_angled12 =[course_gcd_angled12 coursegcd_angled2];
   dist_gcd_angled12 =[dist_gcd_angled12 distgcd_angled2];
end

course_gcd_angled2 =[course_gcd_angled12];
dist_gcd_angled2 =[dist_gcd_angled12];
```

```
% Columns 2,3,5,6,8,9,11,12,14,15,17,18,20,21,23,24,26,27,29,30,32,33,35 and 36
in GCD % matrix
angled_edges1 = [];
for g = 1:length(lon_angled_edges_matrix2(:,1))
    angled_edges2 = [dist_gcd_angled(:,g),dist_gcd_angled2(:,g)];
    angled_edges1 = [angled_edges1 angled_edges2];
end

angled_edges = angled_edges1;

angled_edges_22 = [];
for d = 1:length(angled_edges(1,:))
    angled_edges22 = angled_edges(1:2:end,d);
    angled_edges_22 = [angled_edges_22 angled_edges22];
end

angled_edges_2 = angled_edges_22;

% GCD matrix
GCD2 =[];
for i = 1:length(straight_edges(1,:))-1;
    GCD1 = [straight_edges(:,i), angled_edges_2(:,i+i-1), angled_edges_2(:,i+i)];
    GCD2 = [GCD2 GCD1];
end

GCD = [GCD2 ,straight_edges(:,end)];

% Columns 2,3,5,6,8,9,11,12,14,15,17,18,20,21,23,24,26,27,29,30,32,33,35 and 36
in course % matrix
course_edges1 = [];
for g = 1:length(lon_angled_edges_matrix2(:,1))
    course_edges2 = [course_gcd_angled(:,g),course_gcd_angled2(:,g)];
    course_edges1 = [course_edges1 course_edges2];
end
```

```
course_edges = course_edges1;

course_edges_22 = [];
for d = 1:length(course_edges(1,:))
   course_edges22 = course_edges(1:2:end,d);
   course_edges_22 = [course_edges_22 course_edges22];
end

angled_course_2 = course_edges_22;

% Course matrix
course_matrix2 =[];
for i = 1:length(course_straight_edges(1,:))-1;
   course_matrix1 = [course_straight_edges(:,i), angled_course_2(:,i+i-1),
angled_course_2(:,i+i)];
   course_matrix2 = [course_matrix2 course_matrix1];
end

course_matrix = [course_matrix2 ,course_straight_edges(:,end)];

%% Calculation for GS matrix

windspeed2 = [WindSpeed_matrix_final];
windfrom = [WindDirection_matrix_final];
airspeed = 661.47*Mach_speed*sqrt((K+mean_Temp)/288.15);

% Calculate GS matrix
GS1 = [];
for i = 1:length(GCD(1,:))
[heading, groundspeed, windcorrangle] = driftcorr(course_matrix(:,i), airspeed,
windfrom(:,i), windspeed2(:,i));
GS1= [ GS1 groundspeed];
end
```

```
GS= GS1

%% Calculate the cost ( time per leg in hours )
cost_time = GCD./GS;

%% The adjacency matrix
adj_detailedWeather(:,:);

%% The cost_time adjacency matrix
cost1 = reshape(cost_time',length(cost_time(1,:)),length(cost_time(:,1)));
cost = cost1(:);
cost_t = cost(isfinite(cost(:, 1)), :);
cost_time1 = adj_detailedWeather';
cost_time1(cost_time1==1) = reshape(cost_t',1,numel(cost_t))';
cost_time1 = cost_time1';

% % Shortest path
% Dijktra´s allowing multiple exit points
sparse_cost = sparse(cost_time1);
 h = view(biograph(sparse_cost,[],'ShowWeights','on'))
 [time,path,pred] = graphshortestpath(sparse_cost,1, N-12:N, 'Directed', true,
'Method', 'Dijkstra');

minimum_time =find(time==min(min(time)))
min_time = (N-13)+minimum_time;

[time,path,pred] = graphshortestpath(sparse_cost,1,min_time)

set(h.Nodes(path),'Color',[1 0.4 0.4])
edges = getedgesbynodeid(h,get(h.Nodes(path),'ID'));
set(edges,'LineColor',[1 0 0])
set(edges,'LineWidth',1.5)
```

```
min_time_minutes = time*60

% Difference between actual time and time found using dijktra´s when all
% exit points are allowed
actual_time_flight  =  285.1854;
Improvement_from_actual_timeMinutes  =  actual_time_flight - min_time_minutes;
Improvement_from_actual_time = Improvement_from_actual_timeMinutes
/actual_time_flight % Improvement in percent;

% Dijktra´s only allowing one exit points
 [time,path,pred] = graphshortestpath(sparse_cost,1, (N-6), 'Directed', true, 'Method',
'Dijkstra');

set(h.Nodes(path),'Color',[1 0.6 1])
edges = getedgesbynodeid(h,get(h.Nodes(path),'ID'));
set(edges,'LineColor',[0 1 0])
set(edges,'LineWidth',1.5)

min_time_minutes_oneExit = time*60

% Difference between actual time in fligt and time found using dijktra´s
% and allowing only one exit points
Improvement_from_actual_timeMinutes_oneExit = actual_time_flight -
min_time_minutes_oneExit
Improvement_from_actual_time_oneExit =
Improvement_from_actual_timeMinutes_oneExit /actual_time_flight% Improvement
in percent

%% Calculate fuel saved
 H_p = Flight.Waypoints.Altitude(1);% [feet]
 [T,p,rho,a]=BADAGetISAWeather(H_p,0);
 dT = K + mean_Temp - T; % [K]
 actype = Flight.AircraftType;
 mass = 280010; % [kg]
```

```
 M = Flight.Waypoints.mach_speed(1);
 pitch = 0; % (1 -> climb, 0 -> cruise, -1 -> descent)

[FL, T, p, rho, a, V_TAS_K, V_CAS_K, V_TAS_M, mass, Thrust, Drag, C_L, Fuel,
ESF, ROCD,ROCD_no_red, TDC, PWC] = BADArunModel(H_p, actype, dT, mass,
M, pitch);

Fuel_Burn_perMin = Fuel

% Fuel saved when all exit points are allowed
Fuel_saved_multipleExit = Improvement_from_actual_timeMinutes * Fuel

% Fuel saved when the exit point is fixed
Fuel_saved_oneExit = Improvement_from_actual_timeMinutes_oneExit * Fuel
```

School of Science and Engineering
Reykjavík University
Menntavegi 1
101 Reykjavík, Iceland
Tel. +354 599 6200
Fax +354 599 6201
www.reykjavikuniversity.is
ISSN 1670-8539